HHS Public Access

Author manuscript

Neuroimage. Author manuscript; available in PMC 2018 November 15.

Published in final edited form as:

Neuroimage. 2017 November 15; 162: 199–213. doi:10.1016/j.neuroimage.2017.08.064.

Individual Differences in Regional Cortical Volumes across the Life Span are Associated with Regional Optical Measures of Arterial Elasticity

Antonio M. Chiarelli[~,a], **Mark A. Fletcher**[~,a,b], **Chin Hong Tan**[d], **Kathy A. Low**[a], **Edward L. Maclin**[a], **Benjamin Zimmerman**[a,b], **Tania Kong**[a,c], **Alexander Gorsuch**[a], **Gabriele Gratton**[a,b,c], and **Monica Fabiani**[a,b,c,*]

[a]Beckman Institute, University of Illinois, Urbana, Illinois, USA

[b]Neuroscience Program, University of Illinois, Urbana, Illinois, USA

[c]Department of Psychology, University of Illinois, Urbana, Illinois, USA

[d]Department of Radiology and Biomedical Imaging, University of California, San Francisco, California, USA

Abstract

Aging is often accompanied by changes in brain anatomy and cerebrovascular health. However, the specific relationship between declines in regional cortical volumes and loss of cerebral arterial elasticity is less clear, as only global or very localized estimates of cerebrovascular health have been available. Here we employed a novel tomographic optical method (pulse-DOT) to derive local estimates of cerebral arterial elasticity and compared regional volumetric estimates (obtained with FreeSurfer) with optical arterial elasticity estimates from the same regions in 47 healthy adults (aged 18–75). Between-subject analyses revealed a global correlation between cortical volume and cortical arterial elasticity, which was a significant mediator of the association between age and cortical volume. Crucially, a novel within-subject analysis highlighted the spatial association between *regional* variability in cortical volumes and arterial elasticity *in the same regions*. This association strengthened with age. Gains in the predictability of cortical volumes from arterial elasticity data were obtained by sharpening the resolution up to individual cortical regions. These results indicate that some of the variance of sub-clinical age-related brain atrophy is associated with differences in the status of cerebral arteries, and can help to explain the unique patterns of brain atrophy found within each individual.

[*]Corresponding Author: Monica Fabiani, University of Illinois at Urbana-Champaign, Beckman Institute, 405 N. Mathews Ave., Urbana, IL 61801-2325, mfabiani@illinois.edu, Ph: +1-217-244-1019, Fax: +1-217-333-2922.

[~]Denotes joint first authorship, as each contributed equally to the paper. The two first authors are listed in alphabetical order

Disclosure Statement

The authors declare no actual or potential conflicts of interest. The views expressed in this paper are solely those of the authors.

Keywords

Aging; structural Magnetic Resonance Imaging (sMRI); FreeSurfer; Cerebrovascular health; optical arterial pulse measures (pulse-DOT); Diffuse Optical Tomography (DOT)

1. Introduction

Even in the absence of major clinical pathologies aging is typically associated with changes in brain structure and function. As individuals age, their performance on many cognitive tasks declines (Park et al., 2002; Salthouse, 2010; Schaie, 1989; Wilson et al., 2002). This decline is often accompanied by changes in functional brain activity (Alexander et al., 2012; Andrews-Hanna et al., 2007; Cabeza, 2002; Fabiani, 2012; Fabiani & Gratton, 2012; Hedden & Gabrieli, 2004) as well as by anatomical changes in brain structure (Fletcher et al., 2016; Gordon et al., 2008; Pfefferbaum et al., 2000; Raz et al., 2010). Many factors, however, are thought to contribute to these changes, including genetics, cardiorespiratory fitness levels and nutrition, to name a few (Alexander-Bloch et al., 2013; Erickson et al., 2015; Gómez-Pinilla, 2008; Kramer et al., 2005; Kramer et al., 2006; Monti et al., 2015; Toga & Thompson, 2005; Voss et al., 2013).

Among the factors that can play an important role in mediating the effects of aging on the brain, and explain some of the individual differences that have been observed in this relationship, is the status of the cerebrovascular system. In particular, loss of arterial elasticity is accompanied by cognitive decline (Rabkin, 2012; Unverzagt et al., 2011), can greatly increase the risk of cerebrovascular accidents (Hatanaka et al., 2011; Mattace-Raso et al., 2006), and has been linked to the accumulation of beta-amyloid in Alzheimer's Disease (Casserly & Topol, 2004; Kalaria et al., 2012; see also Hohman et al., 2015). There is also evidence that vascular risk factors may influence brain anatomy and cognitive function even in the absence of stroke or Alzheimer's disease. For instance, Raz and colleagues (2007) showed an association between vascular risk factors, smaller prefrontal volumes, and lower scores on tests of fluid intelligence (see also Jolly et al., 2016; 2017). Similarly, a meta-analysis examining the effects of peripheral blood pressure reported that 26 of the 28 studies included showed an association between hypertension and volumetric reductions in the brain, with particularly strong effects in the frontal and temporal lobes (Beauchet et al., 2013). Although the mechanisms behind these associations are not entirely clear, it is possible that arterial stiffness and/or chronic vasoconstriction may cause chronic brain hypoperfusion, which in turn can lead to brain atrophy, even at sub-clinical levels. Another possibility is that endothelial dysfunction, such as down-regulation of the endothelial growth factor, may play a role in neurodegeneration and cognitive decline (Hohman et al., 2015).

Most of the evidence mentioned above is based on large-scale studies using simple measures of arterial elasticity, such as pulse pressure (i.e., the difference between systolic and diastolic blood pressure), which is known to correlate with systemic arterial stiffness (or inversely correlate with arterial elasticity [Beauchet et al., 2013, Cannesson et al., 2011]). However, pulse pressure tends to be unreliable (Stergiou et al., 2009). Other investigators have used

more precise measures of peripheral arterial stiffness (e.g., pulse wave velocity, augmentation index, ultrasound arterial wall distension), to examine their association with brain and cognitive measures in older adults. Two recent meta-analyses based on studies including these measures provide strong support for an association between peripheral arterial stiffness and declines in cognition, with parallel increases in the number/severity of white matter hyperintensities (Rabkin, 2012; Singer et al., 2014). In contrast, studies of the association between arterial stiffness (measured outside the brain) and volumetric brain changes have provided less clear findings. For instance, a recent study examined the association between overall cortical volume and arterial stiffness (measured as the distension – or lack thereof – of the carotid arteries) using an ultrasound-based wall-tracker system in 526 older participants (Jochemsen et al., 2015; Segers et al., 2004). Although cross-sectional analyses revealed a negative correlation between carotid distension and total gray matter volume (and also a positive correlation with increased white matter lesion volume), these findings did not reach significance in a prospective analysis after a 4-year follow-up. Similarly, a large sample (N=1,223) study of older adults failed to find an association between various peripheral stiffness measures (inverse-transformed carotid-femoral pulse wave velocity, central pulse pressure, and mean arterial pressure) and brain anatomy as a whole (Tsao et al., 2016).

In summary, although these previous studies hint at an association between arterial stiffness and age-related volumetric brain changes, explorations of these associations have been limited in a number of ways. First, most studies have only used peripheral measures of arterial stiffness as an indirect index of cerebral arterial status. Although it is possible that an association between peripheral and cerebral measures exists, there is also evidence (based largely on MR studies) for the existence of a specific pathology of the cerebral vasculature that is to some extent independent from a generalized peripheral vasculature pathology (see for example Blair et al. 2016; Peres et al., 2016; Shy et al., 2016; Van Norden et al., 2011). This underscores the importance of obtaining direct measurements of cerebrovascular status in the brain, which may better correlate with changes to brain anatomy and cognition. Second, the extent to which arterial stiffness mediates the effect of aging on brain anatomy and cortical volume has not been explicitly investigated. Third, due to the fact that peripheral measures only yield a single global estimate of arterial elasticity (or stiffness) per individual, comparisons between *regional* cerebral arterial stiffness and *regional* gray matter volumes have not been possible. An important aspect of anatomical brain changes in aging is that different regions do not lose tissue homogenously across the lifespan. Although some regions are more affected by aging than others (Fjell et al., 2013; Walhovd et al., 2011), the exact spatial distribution and magnitude of these changes varies across and within individuals (Alexander-Bloch et al., 2013; Gordon et al., 2008; Raz et al., 2010). Furthermore, the mechanisms underlying the increased sensitivity of certain brain regions to aging are not fully known (Fletcher et al., 2016). A possible cause of individual variability in the spatial distribution of brain atrophy may be that the spatial patterns of integrity of the local vascular system might also differ across individuals, and influence the degree of atrophy regionally.

To overcome these limitations, we recently developed a new procedure to assess local cerebrovascular health using near-infrared (NIR) light (Fabiani et al, 2014; Tan et al., 2016;

see also Tan et al., 2017). This technique involves injecting NIR light through the scalp and detecting the backscattered light at a certain distance from the light source. The pulsation of blood in the arteries and arterioles produces large periodic changes in oxy-hemoglobin concentration, which cause oscillations in the amount of light absorbed by the tissue. These changes are commonly measured in the finger using photoplethysmography (i.e., pulse oximetry). In the brain, pulsation data can be easily obtained using the same procedures employed for functional near infrared spectroscopy (fNIRS; Hoshi & Tamura, 1993; Murkin & Arango, 2009; Villringer & Chance, 1997). The optical arterial pulse obtained in this fashion is a very large signal, easily identifiable in each individual subject and at each recording location without averaging, although even greater reliability can be achieved by averaging over a few minutes of recording (Fabiani et al., 2014; Tan et al., 2017).

When the focus is on functional brain imaging (fNIRS), the pulse signal is eliminated as a nuisance variable (Gratton & Corballis, 1995), whereas here we use it as the signal of interest. In previous work, we have demonstrated that the optical pulse signal comes from arteries inside the skull rather than from superficial, extracranial, head arteries (Fabiani et al., 2014)[1]. We have also shown that various parameters related to cerebral arterial health can be extracted from the recorded optical pulse, including measures of pulse pressure, transit time (or pulse wave velocity), and a measure of the shape of the pulse that we label here pulse relaxation function, or PReFx (previously labeled arterial compliance; see Fabiani et al., 2014; Tan et al., 2017).[2] According to the Windkessel model, healthy elastic arteries enable slower pulse wave velocity and delayed recoil, allowing for a temporally distributed pulse wave and for sustained blood flow even during the diastolic period (Izzo & Shykoff, 2001). Conversely, stiff arteries result in increased pulse wave velocity and quick recoil, thus generating a large pulse response during the systolic period, but reduced ability to maintain a prolonged blood flow during the diastolic period. This difference implies a smaller and smoother optical pulse from healthy arteries when compared to stiff ones, which yield a larger and “spikier” response. Thus the degree of arterial elasticity in brain arteries and arterioles can be assessed by measuring the shape of the arterial pulse, and in particular by the extent to which the artery retains its expanded volume after the systolic peak. The pulse relaxation function (PReFx) measure (see Figure 1b) reflects a combination of arterial elasticity and peripheral resistance. The Fabiani et al. (2014) study was the first to demonstrate that this parameter was negatively correlated with age and positively correlated with cardiorespiratory fitness in a group of healthy older adults between the ages of 55 and 87. Most importantly for the purposes of this paper, PReFx was positively correlated with overall brain volumes (total gray, white and subcortical gray matter) as well as with measures of cognitive flexibility. A recent replication examining these measures across the life span in an independent sample (ages 18–75) demonstrated the excellent reliability of

[1]We have used four criteria to ascertain that this is the case: (1) large arteries are spatially localized consistently with intracranial, rather than extracranial arteries; (2) the arterial flow and timing of pulse peak (measured by pulse transit time at different locations along a large artery) are consistent with intracranial rather than extracranial arteries; (3) local optical pulse measures are predictive of phenomena (cortical atrophy and/or cognitive deficits) that are specific to those same brain areas; and (4) the pulse parameters are very similar when obtained using light intensity and phase delay methods, which should produce similar effects for signals generated in deep (>1 cm) head locations, but opposite effects for signals generated in superficial (<1 cm) locations.

[2]In previous publications (e.g., Fabiani et al., 2014) we have referred to this pulse shape measure as “arterial compliance”. However, since this term is also used to refer to a different phenomenon (i.e., the amount of arterial distension as a function of arterial pressure change), we are now using the more descriptive term “pulse relaxation function” (and the corresponding acronym PReFx).

these measures and replicated the positive association found between PReFx and measures of global brain anatomy (Tan et al., 2017).

In this paper, we have extended these optical measures of arterial stiffness by implementing a diffuse optical tomography (DOT) approach (Chiarelli et al., 2016). This procedure produces 3D images of the optical pulse (or pulse-DOT) within the head, allowing us to better explore the spatial relationship between optical measures of arterial stiffness and measures of cortical volume (derived from structural Magnetic Resonance Imaging, sMRI, using FreeSurfer©) across cortical regions for each participant. Although the pulse-DOT measures can in principle be used to investigate a number of pulse parameters within the brain (such as pulse amplitude and pulse transit time), here we focused on PReFx. This parameter was selected because it is less influenced by the presence of larger arteries (which can impact pulse amplitude, a proxy for pulse pressure), and is not impacted by its distance from the carotids (which influences pulse transit time; Fabiani et al., 2104). Both of these characteristics are useful when comparing arterial pulse parameters across brain regions and subjects. We measured the average arterial PReFx for each of 50 regions of interest (ROIs) that were defined using the Desikan-Killiany atlas of FreeSurfer (Desikan et al., 2006), separately for each subject. We then examined (1) the association between global arterial elasticity and overall cortical volumes; (2) the mediation value of PReFx in explaining the relationship between age and global variations in brain anatomy; and (3) the associations between regional arterial elasticity and regional cortical volume and how they may change with aging.

2. Method

2.1 Participants

Participants in this study were the same as in Tan et al. (2017). However, this study includes, for the first time, tomographic reconstruction of the optical arterial data, mediation analyses focused on overall brain anatomical data, and analyses of the *regional* relationship between optical and structural MRI data (the central focus of the current study), none of which was included in Tan et al. (2017).

Forty-eight healthy adults (25 females) between the ages of 18 and 75 years were recruited for participation in the study. Participants were recruited in a stratified manner in order to obtain a final sample of relatively equal numbers of men and women within each age decade. The study was approved by the Institutional Review Board of the University of Illinois and participants signed informed consent. Participants admitted into the study reported themselves free of serious health problems, including mental or neurological disease, and other serious chronic medical conditions such as diabetes. All participants were right-handed as assessed by the Edinburgh Handedness Inventory (Oldfield, 1971) and native speakers of English. Other criteria for inclusion were to be free of dementia (i.e., having a score of 50 or higher on the modified Mini-Mental Status Exam; Mayeux et al., 1981) and depression (as assessed by the Beck's Depression Inventory; Beck & Steer, 1987). One participant was excluded from all analyses due to problems in optical data collection, leaving a total of 47 participants (24 females).

Average demographics, including age, BMI and blood pressure are reported in Table 1. A median-split-by-age analysis indicated that the older group had on average a higher level of education compared to the younger group. However, it is important to note that many of the youngest participants were not old enough to have completed undergraduate or graduate education. All other measures (except age) were not statistically different between the two groups.

2.2 Collection and processing of structural MRI data

Structural magnetic resonance images (sMRI) were collected for each participant using a 3T Siemens Trio full body scanner. A high resolution, 3D MPRAGE protocol was used, with a flip angle = 9°, TE = 2.32 ms, TR = 1900 ms, and inversion time = 900 ms. Slices were obtained in the sagittal plane (192 slices, .9 mm slice thickness, voxel size .9 × .9 × .9 mm) having matrix dimensions of 192 × 256 × 256 (in-plane interpolated at acquisition to 192×512×512) and field of view of 172.8 × 230 × 230 mm.

FreeSurfer© 5.3 (Dale et al., 1999; Fischl & Dale, 2000; Fischl et al., 2001; Fischl et al., 1999a; Fischl et al., 1999b; Fischl et al., 2004) was used to extract cortical ROIs for each participant. All FreeSurfer output was visually inspected by two trained reviewers and errors were corrected according to standard methods recommended by the Martinos Center for Biomedical Imaging (for additional information, see https://surfer.nmr.mgh.harvard.edu/fswiki/FsTutorial/TroubleshootingData). After error correction, the Desikan-Killiany atlas was used to define cortical ROIs for each individual, and cortical volume was estimated for each of these regions (see Desikan et al., 2006, for ROI visualization). To account for differences in head size volumes were normalized by the estimated intracranial volume provided by FreeSurfer 5.3 using the method first described by Jack et al. (1989). Lastly, to estimate the size of the cortical volume of each ROI of a given subject relative to the mean and standard deviation across all other subjects, the ROI volume estimates were standardized (i.e., mean=0 and SD=1) across participants, but within each region; this also allowed us to account for baseline differences in the size of the different atlas-defined ROIs. In addition to measures of cortical volume, estimates of cortical thickness were obtained for each ROI and subjected to the same normalization procedures used for the volume estimates.

2.3 Electrocardiogram recording and analysis

The electrocardiogram (EKG) was recorded with a Brain-Vision™ recorder and a Brain-Vision professional BrainAmp™ integrated amplifier system (Brain Products GmbH, Germany), in order to synchronize the optical pulse data to the R wave of the EKG and ensure that the same pulse was examined regardless of location. Specifically, lead I of the EKG (left wrist referenced to right wrist) was recorded with a sampling rate of 200 Hz and a band-pass filter of 0.1 Hz to 100 Hz. The exact timing of each R-wave peak was found by searching for peak points exceeding a certain voltage threshold (scaled for each participant) and dismissing any peak points outside the normal range of inter-beat intervals. Proper identification of each peak was subsequently ensured by visual inspection and false detections (e.g., a large T wave inadvertently identified as an R wave) were eliminated (these were very rare, <5%).

2.4 Optical recordings

Optical data were acquired with a multi-channel frequency-domain oximeter (ISS Imagent™, Champaign, Illinois) equipped with 128 laser diodes (64 emitting light at 690 nm and 64 at 830 nm) and 24 photo-multiplier tubes (PMTs). Time-division multiplexing was employed so that each detector picked up light from 16 different sources at different times within a multiplexing cycle. The sampling rate was 39.0625 Hz. The light was carried to the scalp using single optic fibers (0.4 mm core) and from the scalp back to the detectors using fiber bundles (3 mm diameter). The fibers were held in place using soft, but rigid, custom-built helmets, whose sizes differed as a function of head circumference. During the recording, participants performed a resting-state paradigm (e.g., Eggebrecht et al., 2014): Two 6-minute blocks were recorded for each of four consecutive recording sessions in which different optical recording montages were used, spanning a recording period of approximately 3 hours (including the time required for setting up new optical montages). The helmet was never removed across the whole optical recording. A total of 384 channels (192 at 830 nm and 192 at 690 nm) were acquired for each montage, with source-detector distances varying between 15 mm and 80 mm for a total of 1536 channels covering most of the scalp surface. The optical measurements were based on a high density, large field-of-view optode montage (covering the majority of the cortical mantle). Figure 1a shows source and detector locations, and the area of optical sensitivity given the newly implemented tomographic approach, rendered onto the structural MR image of a representative participant.

2.5 Optode digitization and MRI co-registration

While the helmets were still sitting on the subjects' head, fiducial markers were placed on their left and right pre-auricular points (LPA and RPA) and on the nasion (Na). These fiducial points, optode locations, and other scalp locations were digitized with a Polhemus FastTrak 3D digitizer (Colchester, VT; accuracy: 0.8 mm) using a recording stylus and three head-mounted receivers, which allowed for small movements of the head in between measurements. Optode locations and structural MRI data were then co-registered using the fiducials and a surface-fitting Levenberq and Marquard algorithm (Chiarelli et al., 2015b; see also Whalen et al., 2008).

2.5 Optical pulse analysis

The optical DC intensity data (i.e., average measures of the amount light produced by a specific source and reaching a particular detector during a multiplexed 1.6-ms interval) were normalized (by dividing them by their mean value), movement corrected (Chiarelli et al. 2015a), and band-pass filtered between 0.5–5 Hz (Butterworth digital filter). As arterial blood is highly (>95%) saturated, only light intensity data at 830 nm of wavelength were used for pulse shape estimation. The longer 830-nm wavelength has a higher sensitivity to pulse-related absorption changes due to its higher sensitivity to oxygenated hemoglobin when compared to the shorter 690-nm wavelength (Fabiani et al., 2014). The use of one wavelength (rather than two) facilitated the tomographic (3D) reconstruction process. However, in our past work, we found a very strong correlation (r>.95) between pulse measures obtained using 690 nm and 830 nm light (Fabiani et al., 2014).

The pulse waveform for each channel was obtained by averaging the DC light intensity time locked to the peak of the R wave of the EKG (signaling the depolarization of the ventricular myocardium), ensuring that the same pulse cycle was measured at all locations. To determine the reliability of pulse parameters, data for the first and second recording block (for each optode montage) were averaged separately, and separate estimates of optical parameters were obtained for each block. For all other analyses the averages obtained from the two blocks were collapsed. In order to decrease sensitivity to superficial artifacts, only channels with inter-optode distance >25 mm were used. To increase the overall signal-to-noise ratio (SNR) of the measurements channels with inter-optode distance >70 mm were not used, as they provide levels of light that are too low to be useful.

In order to generate a 3D reconstruction of the pulse waveform across the head, a model of light propagation within the head (forward model) and an inverse procedure are required. The Finite Element Method (FEM) applied to the diffusion equation (Ishimaru, 1989; Paulsen & Jiang, 1995) was used to estimate the forward model. The FEM software NIRFAST (Dehghani et al., 2009; Eggebrecht et al., 2014) was used to model light propagation through heterogeneous head models and to compute Jacobian (sensitivity) matrices of DC light intensity reflecting absorption changes. Figure 1a reports an example of an average Jacobian (average optical sensitivity) for a representative participant overlaid onto the same participant's anatomical MRI. The average Jacobian is displayed up to an attenuation of 60 dB (1000 times) from its maximum value. "Fine" meshes (maximum tetrahedral volume = 2 mm^3) were generated for FEM using the Matlab software *iso2mesh* (Fang & Boas, 2009). The heterogeneous head models were based on segmented T1-weighted 3D anatomical images. Segmentation of the skull and scalp, cerebrospinal fluid (CSF), white matter, and gray matter was performed using Statistical Parametric Mapping (SPM, Friston et al., 1994) functions applied to T1 weighted images (Penny et al., 2011). Baseline optical properties (absorption μ_a, reduced scattering coefficient μ_s' and refraction index η) of the tissues at the relevant wavelength were taken from Tian and Liu (2014) and Chiarelli et al. (2016). The optical values at the wavelength of interest (830 nm) were set to: scalp and skull: $\mu_a = 0.014\ mm^{-1}$, $\mu_s' = 0.84\ mm^{-1}$; CSF: $\mu_a = 0.004\ mm^{-1}$, $\mu_s' = 0.3\ mm^{-1}$; grey matter: $\mu_a = 0.019\ mm^{-1}$, $\mu_s' = 0.673\ mm^{-1}$; white matter: $\mu_a = 0.021\ mm^{-1}$, $\mu_s' = 1.01\ mm^{-}$. The refraction index was set at $\eta = 1.4$ for all the simulations and mediums considered. An inverse procedure introduced by Chiarelli et al. (2016) was used to convert intensity changes on individual channels to absorption changes in voxel space. This inverse procedure allowed for an unbiased localization of absorption fluctuations up to a depth of 30 mm from the scalp.

PReFx (see Figure 1b and Fabiani et al., 2014; Tan et al., 2017) is a measure of the shape of the pulse during the interval between a peak systole and a peak diastole. It describes the way in which arteries return to their original size after dilating to accommodate the blood bolus generated by a heart pulsation. To the extent that this curve is decelerated, the artery can be considered to be elastic; acceleration of this function is a sign of arterial stiffness (Oliver & Webb, 2003). For this reason, PReFx is computed as the area under the pulse during this interval, after subtraction of a triangle describing a "linear" relaxation. To make this measure independent of peak amplitude (which is related to pulse pressure) and heart rate, the values

are normalized (setting the peak systole = 1 and peak diastole = 0; and dividing them by the duration of the systole-diastole interval)[3].

PReFx was estimated for each voxel for which the sensitivity (measured by the average Jacobian) was greater than 1/1000 (60 dB) of the maximum value. This allowed us to disregard voxels too deep to provide useful data (approximately > 3 cm from the scalp) as well as voxels that were not covered by the optical montage (Figure 1a). In addition, only voxels within the cortex (as identified by FreeSurfer) were considered. *Regional* PReFx was computed for 50 of the 70 FreeSurfer regions (25 from each hemisphere). These regions were selected because, on average, at least 10% of their volume was sampled by the optical recording (note that for all subjects, optical estimates were available for at least 5% of the voxels for all these areas). The other 20 regions (10 per hemisphere) did not satisfy these criteria because they were either too deep or insufficiently covered by the optical montages. As such, reliable measurement of the pulse and PReFx could not be obtained for these regions. Regional PReFx was estimated as the average PReFx across the voxels included in the ROI for which optical estimates of the pulse were available. The 50 ROIs used for pulse measurement are listed in Table 2.

2.6 Statistical and mediation analyses

Since most of our a-priori hypotheses were directional (as we expect that greater arterial elasticity will be associated with larger volumes and younger ages), one-tailed *p*-values are reported (unless noted otherwise). To further investigate the effects of age, follow-up analyses typically involved a median split of the whole sample based on age (over or under the age of 48).

A mediation analysis was performed in order to determine whether arterial elasticity (as measured with PReFx) acts as a mediator on the relationship between age and global volume. This analysis was performed using model four of the PROCESS macro for SPSS (Hayes, 2008). This tool generates a bootstrapping distribution to empirically estimate a confidence interval for the mediation effect. This, in turn, allows us to determine if an intervening variable (in this case PReFx) significantly weakens or suppresses (mediation) an existing association between an independent (age) and dependent (volume) variables. All analyses were performed both with and without removing the variance accounted for by systolic and diastolic pressure. The analyses were based on 10,000 bootstrap samples and a 95% confidence interval (see Zimmerman et al., 2014 for a similar approach).

2.7 Hierarchical clustering

A data-driven clustering procedure was implemented in order to test the level of spatial specificity in the relationship between cortical volume and PReFx. To this end we first performed a hierarchical agglomerative (bottom-up) clustering (Corpet, 1988), starting from 50 clusters (i.e., each segmented FreeSurfer region) and 47 participants. The Euclidean metric and the Ward's method (Ward, 1963) were used for the clustering procedure. This method decreases the number of clusters (which means fusing previous clusters) by

[3]Note that this calculation might lead to a negative number, although this never occurred within this dataset.

minimizing the total within-cluster variance. The cluster analysis was performed separately for standardized volume and PReFx data. We were then interested in determining whether progressively smaller clusters would provide a better depiction of the relationship between cortical volume and PReFx. This was based on analyzing how much of the total variance in cortical volumes observed between different regions occurred between clusters defined on the basis of PReFx, as the size of the clusters progressively diminished (or as the number of clusters progressively grew). In principle this problem can be considered akin to a multiple regression analysis, in which the ability of a model (in this case, a cluster-based classification of brain regions based on arterial elasticity) to predict variance in a dependent variable (in this case, cortical volume for each region) can be expected to increase as the number of predictors (i.e., clusters) increases, although this may occur as a function of chance. We therefore applied a correction function (normally used in multiple regression) to account for the effect of chance. We then examined how much additional variance was accounted for by the model every time we increased the number of clusters (in this case, in steps of four). The size of each step (4) was empirically chosen to be a compromise between noise level and resolution of the clustering test. To determine whether this increase was significant, we computed an F ratio between the additional between-cluster variance obtained by incrementing the number of clusters by 4 and the residual error variance (updated for each level of the model), with each term divided by the appropriate degrees of freedom. This method was used to identify the levels along the hierarchy of clustering steps that actually provided a significant increase in the amount of variance in cortical volume accounted for.

3. Results

3.1 Reliability of PReFx estimates and relationship with heart rate

The reliability of the PReFx estimates (averaged across the 50 ROIs), calculated as the across-participants correlation between the values obtained for the first and second recording block, was extremely high ($r(45)=0.98$, $p<.0001$). Importantly, PReFx was not significantly correlated (across subjects) with the average heart rate obtained during the measurement ($r(45)=-0.11$, *n.s.*). This suggests that our normalization procedure was successful, and that PReFx is a measure of pulse shape, independent of the inter-beat interval (i.e., the inverse of heart rate).

3.2 Global arterial elasticity and brain volume, and related mediation analysis

We computed the average cortical volume and average PReFx across all 50 ROIs. Across the 47 subjects, global PReFx had average value of 0.101 (SD=0.044). The highest value of PReFx was 0.237, obtained for a 20-years-old participant, whereas the lowest value was 0.021 in a 60-years-old participant. A two-way ANOVA was performed on both cortical volume and PReFx considering age and sex as factors. Both volume and PReFx results showed strong main effects of age ($F(1,43)=39.76$, $p<.001$, $F(1,43)=8.65$, $p<.01$, respectively) but no significant main effect or interactions involving sex. Thus, to conserve degrees of freedom, the analyses involving these two variables were not adjusted for sex.

On average, both cortical volume and PReFx significantly declined with age, $r(45) = -.82$ and −.46, respectively, p's<.001. Moreover, there was a positive correlation between PReFx and grey matter volume, $r(45)=.54$, $p<.001$. Cortical thickness estimates (averaged across regions) also correlated with both age and PReFx, albeit to a lesser extent than volume ($r(45) = -.65$ and −.43, respectively, p's<.01).

Since it was hypothesized that part of the age-related reduction in brain volume is due to arterial stiffness, it is important to determine whether PReFx acts as a significant mediator of these age-related effects on global brain volume. To address the first question, we performed a mediation analysis (Hayes, 2008). As can be seen in Figure 2, this analysis showed that PReFx significantly mediated the association between age and volume (the 95% confidence interval of the Interference Indirect Effect ranged between −.0313 and −.0186, N=47, Bootstrap=10,000). This mediation also remained significant when controlling for both systolic and diastolic blood pressure (the 95% confidence interval of Interference Indirect Effect ranged between −.0078 and −.0004) suggesting that PReFx provided additional explanatory power for the relationship between age and total brain cortical volume, over and above that provided by systemic pulse pressure measures.

An alternative hypothesis is that the correlation between PReFx and global brain volume is spurious, only reflecting the correlation between PReFx and age. To address this hypothesis, we performed a step-wise multiple regression analysis in which age was partialed out before computing the correlation between arterial PReFx and global brain volume. The residual partial correlation was still significant, $r(45)= 0.319$, $p<.05$, indicating that the relationship between overall PReFx and global brain volume is not simply due to its relationship age.

3.3 Regional arterial elasticity and cortical volume

The main purpose of this paper is to explore the regional (rather than global) relationships between cortical volumes and arterial elasticity. For that we computed correlations between age and cortical volume, age and PReFx, and PReFx and cortical volume for each of the 50 ROIs. Maps of these correlations (in which correlations are presented in the form of a color scale for each cortical ROI) can be seen in Figure 3. For display purposes, we used a color scale based on the absolute (unsigned) value of the correlation coefficients (as correlations between age and volume and age and PReFx are expected to be negative, whereas correlations between PReFx and volume are expected to be positive). The findings indicate that, in our sample, age-related atrophy is particularly evident in frontal, parietal and temporal regions, with a smaller degree of atrophy in occipital regions. Interestingly, a similar spatial pattern can be found for the other two sets of correlations (age vs. PReFx and PReFx vs. cortical volume), indicating that the average spatial distribution of these regional effects is similar. To quantify the visual similarities across these maps, we computed spatial correlations to evaluate their overlap in an ROI-wise fashion. The spatial correlation between the age/volume and PReFx/volume correlations was $r(48)=0.33$, $p=0.017$, that between age/volume and age/PReFx was $r(48)=-0.36$, $p=0.001$, and that between age/PReFx and PReFx/volume was $r(48)=-0.65$, $p<.0001$.

3.4 Spatial relationship between arterial elasticity and cortical volume: Hemispheric analysis

As a first step to assess the spatial association between regional vascular and volumetric measures within each participant, we examined the relationship between hemispheric differences in cortical volume and hemispheric differences in PReFx. Across all participants (Figure 4a) there was a significant positive association between the hemispheric patterns of PReFx and cortical volume ($r(45)=.24$, $p<.05$), indicating that the hemisphere with higher PReFx also had greater cortical volume (or less atrophy). This relationship was, however, primarily driven by the older (>48) adults. Figures 4b and 4c show that when younger and older adults are considered separately, the spatial relationship between PReFx and volume was only significant for the older group (young, $r(21)=.13$, ns ; old, $r(22)=.41$, $p<.05$).

3.5 Spatial relationship between arterial elasticity and cortical volume: ROI analysis

To examine the association between regional variations in arterial elasticity and regional volumetric patterns, for each participant we computed the spatial correlation (across the 50 ROIs) between PReFx and brain volume. Each participant's spatial correlation was then Fisher transformed. A *t*-test revealed that the spatial relationship was significantly different from zero when considering all participants, $t(46)=2.70$, $p<.01$ (see Figure 5a, dark grey bar). Similarly to the global analysis, a two-way ANOVA was performed using the regional correlations between cortical volume and PReFx as the dependent variable and age and sex as factors. Results indicated a significant main effect of age ($F(1,43)=18.14$, $p<.001$) but no significant main effect or interactions involving sex. Therefore, to conserve degrees of freedom, the analyses were not adjusted for sex.

An identical analysis was also performed on younger and older adults separately (Figure 5a, white and light gray bars, respectively). This analysis revealed that the spatial relationship was driven primarily by the older half of the participants (age > 48, $t(23)=5.17$, $p<.001$), with no significant difference from 0 seen within the younger adults (age < 48, $t(22)= -.58$, ns). This analysis suggests that the association between arterial elasticity (PReFx) and volumetric patterns within individuals becomes stronger with age. In support of this notion, age and the strength of the spatial relationship were found to be positively correlated, $r(45)=.44$, $p<.01$ (Figure 5b).

A similar analysis was conducted on the spatial relationship between arterial elasticity and cortical thickness. Compared to PReFx-cortical volume analysis, the results were generally similar in direction, but weaker (not reaching statistical significance): for all participants, $t(46)=0.23$, *n.s.*; for the younger group, $t(22)=-1.16$, *n.s.*; for the older group, $t(23)=1.64$, *n.s.*; correlation between age and strength of the spatial relationship, $r(45)=.15$, *n.s.*

3.6 Spatial relationship between arterial elasticity and cortical volume: Cluster analysis

The presence of an age-related correlation between regional PReFx and regional cortical volume implies that localized measures of PReFx may contain useful information (at least in terms of predicting brain atrophy) over and above arterial pulse measures taken at the carotids or peripherally. However, an important question is left unanswered: How local are these effects? Is there additional information provided by the regional measures of PReFx

beyond what can be obtained by separately measuring it in the left and right hemisphere? To address this question it may be useful to assess: (a) whether the PReFx maps provide reliable *regional* information (at a scale smaller than the hemispheric distinction); (b) whether a corresponding specificity in atrophy exists in cortical volumes; and (c) whether the level of correspondence between PReFx and cortical volume is maintained, or even increases, when progressively smaller areas of the cortex are examined. These questions are particularly relevant because optical arterial pulse data may possess a lower spatial resolution than structural MRI data, and because the degree of independence of local PReFx estimates is largely unknown. To address these issues, we employed a clustering algorithm to group those ROIs whose PReFx (or cortical volume) tended to vary together. By using this clustering procedure we were able to group ROIs into increasingly larger clusters – corresponding to decreasing spatial resolution.

Figure 6 reports the data obtained in the cluster analysis. The top portions of figure 6a (clustering by volume) and 6b (clustering by PReFx) show the results of the cluster analysis in the form of dendrograms. The heights of the dendrograms' branches represent the distances (based on the metric employed) between the different regions/clusters. Each row of each matrix represents an individual participant, with participants ordered by age in years from younger (top) to older (bottom), and color indicating their volumetric (6a) and PReFx (6b) rankings in *z* scores for each brain area (columns, reordered as a function of the results of the cluster analysis). Note that for both cortical volume and arterial PReFx higher *z* scores (reds) tend to appear in the upper sections of the matrices (younger subjects), and smaller z scores (blues) tend to appear in the lower sections (older adults), mirroring the global analyses (which show that younger adults have larger volumes and greater PReFx than older adults). Figure 7 reports a map of the effects of a particular level of clustering in which the 50 ROIs are grouped into 6 separate clusters on the basis of the PReFx measures. Colors in this figure denote the separate ROI clusters. This figure indicates that the 6 clusters were largely composed of adjacent and/or hemispherically symmetrical regions. Note that the clustering is completely data driven and does not include any information about the spatial location of the original regions.

Crucially for these regional analyses, subjects (rows in figure 6) show clear individual variability in *z* score values for different brain areas for both regional volumes and regional PReFx. The analyses presented earlier (Figure 5) indicate that, within each subject, variability in each of these two measures tends to be correlated in older, but not in younger adults. For application purposes, it is important to determine which level of clustering optimally supports this correlation, that is, which level of PReFx clustering provides the most useful information about variations in cortical volume. To this end, we started by considering how much of the total variance in cortical volume (R^2) was accounted for by clustering models with progressively more (and smaller) clusters (Figure 8a). Not surprisingly, this value increases with the number of clusters, with $R^2=1$ when the number of clusters equaled the number of ROIs – a result that could be expected even based on chance alone. We therefore corrected this value for the increase in number of clusters (using the formula normally applied to multiple regression to correct the multiple R^2 for the effect of increasing number of predictors). We then examined the differential increase in R^2 as a function of using an increasing number of arterial PReFx clusters (in steps of four) for

predicting cortical volume (Figure 8b), and applied an extra sums-of-square logic based on *F* ratios between the predicted and error variances to determine which increases were significant (Figure 8c). Specifically, Figure 8c reports the results of a series of extra sums-of-square tests (in the form of F ratio values) for increments in between-cluster cortical volume variance (steps of 4 clusters), plotted as a function of the number of clusters (continuous line). To establish the significance of these increments, we used a non-parametric Monte Carlo approach. In the figure, the dashed line shows the 95% confidence interval of the F ratio values for each clustering level.

The results shown in Figure 8c indicate that there is a significant increase in the variance of cortical volume accounted for by arterial elasticity when the arterial elasticity clusters are increased from 1 up to 7 ($p<0.05$), and a second interval of significant increase when between 17 and 19 clusters are considered ($p<0.05$). This indicates that there is added value in predicting cortical volume from arterial PReFx, not only when we consider separate PReFx values for the two hemispheres, but also when we further subdivide the values of arterial PReFx into smaller clusters. It should be noted that it is not clear whether this is the actual upper limit in terms of the number of clusters that it would be profitable to consider. In fact, the statistical power of the analysis drops when we increase the number of clusters (given the number of participants in this study), and the limit of 19 clusters may just reflect this progressive decrease in power. In any case, the data strongly support the idea that the relationship between arterial elasticity (PReFx) and cortical volume is not just due to inter-hemispheric phenomena, but can be observed even within each hemisphere, within each lobe, and possibly within smaller adjacent regions.

4. Discussion

In this study we sought to investigate whether *regional* variations in brain volumetric estimates were associated with variations in arterial elasticity in the same regions. This was enabled by newly developed diffuse optical methods (pulse-DOT) to estimate parameters of arterial elasticity (PReFx) over the entire cortical mantle. To briefly summarize our main findings: first and consistent with previous reports (Fabiani et al., 2014) we showed that *tomographic* measurements of arterial elasticity, averaged across all cortical regions, are strongly associated with age and cortical volume; second, we showed that arterial elasticity is a significant mediator of the relationship between aging and cortical volume; and third, we showed the existence of a spatial overlap between regions with low arterial elasticity and those with small cortical volumes, a relationship that emerges in older adults (>48 years old) but it is not apparent in younger adults.

4.1 Methodological Innovations

The relationship between vascular health and brain anatomy has been previously investigated using systemic (largely peripheral) measures of arterial status (Beauchet et al., 2013; Jochemsen et al., 2015; Rabkin, 2012; Raz et al., 2008; Singer et al., 2014; Tsao et al., 2016). However, there is now considerable evidence that the cerebrovascular system may present specific alterations and pathologies with aging, which are somewhat independent of those observed in the rest of the body. Examples of such pathologies are small vessel brain

disease (Blair et al., 2016, Van Norden et al., 2011) and cerebral amyloid angiopathy (Biffi & Greenberg, 2011). This suggests that the direct measurements of arterial pulse parameters in the cortex provided by the pulse-DOT measures used in the current study could potentially be useful for clinical purposes.

Optical methods have been used clinically to study pulse parameters and blood oxygenation in the periphery for decades (e.g., photoplethysmography/pulse oximetry; Alian & Shelley, 2014; Allen, 2007) and have been shown to yield waveforms very similar to those obtained with continuous-wave Doppler (Cook, 2001; Wisely & Cook, 2001). Our recent studies (Fabiani et al., 2014; Tan et al., 2017) demonstrated for the first time that it is possible to measure the optical pulse over the entire cortical surface. In this paper we further expanded this approach by generating *tomographic* maps of the shape of the pulse across much of the cortex. Specifically, we combined a recently developed 3D reconstruction method for diffuse optical imaging (Chiarelli et al., 2016) with parcellation of anatomical volumes obtained with FreeSurfer to specify the regional relationship between cortical atrophy and arterial elasticity (measured using the PReFx parameter) in a cross-sectional sample encompassing a broad age range (18–75 years). It is important to note that the inherent SNR of the measurement is very high. In fact, pulse propagation in the arteries causes a relative signal change of 1–2%, which is at least one order of magnitude higher than the recording noise of the current instrumentation. This high SNR is further enhanced by averaging pulses over a few minutes of recording, as demonstrated by the very high reliability of the PReFx estimates obtained in the current study ($r > .98$, when 3D-reconstructed and averaged across the whole head).

Other methods can be used to measure pulse parameters directly in the head. For instance, transcranial Doppler can be used to assess the status of particular locations along selected cerebral arteries, such as the middle cerebral artery (MCA; Aaslid, 2012). Similarly, another recently developed method based on MR arterial spin labeling (ASL; Yan et al., 2016) has made it possible to estimate the effects of vascular compliance in targeted head slices. Although neither of these methods is suitable for generating maps of arterial function that explore extended regions of the cortex, they can be used to examine specific arteries, including deep arteries that are not visible with pulse-DOT (depth ≈ 3 cm; Chiarelli et al., 2016). Thus these techniques are best viewed as complementary, given the feasibility of concurrently recording pulse-DOT and MRI or sonography data.

It should be noted that the pulse shape measured with PReFx is influenced by both arterial elasticity – which in large part determines pulse wave velocity – and the presence of peripheral resistance – which determines the occurrence of a recoil wave, traveling opposite to the forward pulse wave. To the extent that (a) there is peripheral resistance, and (b) pulse wave velocity is slow, the pulse relaxation curve will be decelerated and PReFx measure will be positive. Lack of any peripheral resistance and/or fast pulse wave velocity will result in an accelerated pulse relaxation curve and a negative PReFx measure. In the current paper we have assumed that peripheral resistance is relatively constant, and that therefore PReFx only reflects pulse wave velocity (and therefore arterial elasticity). This assumption simplifies the interpretation of the data and is consistent with all the results – but it may not be always correct. Future research on the effects of variations in peripheral resistance (as, for instance,

under conditions of peripheral vasodilation or vasoconstriction) on the PReFx parameter may help clarifying this issue.

4.2 Relationship between arterial elasticity and cortical volume

The data reported in this paper replicate findings by Fabiani et al. (2014), indicating that overall cerebral arterial elasticity (as measured by PReFx) is a significant correlate of between-subject variations in global cortical volume. Here we also show that arterial elasticity measured in the brain successfully mediates the relationship between age and brain volume, even when controlling for systolic and diastolic blood pressure, suggesting that pulse-DOT measures provide additional information compared to peripheral indices of arterial elasticity such as pulse pressure. In line with previous reports (Gordon et al., 2008; Beauchet et al., 2013, Fjell et al., 2013; Walhovd et al., 2011), our data also indicate that certain areas of the brain (such as frontal, parietal and temporal regions) appear to be more susceptible to the effects of aging than other regions for both volumetric and arterial elasticity measures (Figure 3, top and middle rows).

In this paper, we then investigated for the first time the extent to which *intra-individual* variability in cortical volume across regions is associated with a corresponding intra-individual, across-region variability in arterial elasticity. Two levels of this regional specificity were considered: hemispheric and ROI-based. At both levels of analysis, the data revealed that local variations in arterial elasticity are associated with local variations in cortical volume. In other words, within the same individuals, those regions that have a more compromised arterial elasticity are also the regions with more compromised cortical volume.

This phenomenon highlights the importance of arterial elasticity in the maintenance of a healthy brain. Although it was previously known that extreme narrowing and/or stiffening of cerebral or peripheral arteries can lead to cerebrovascular problems (e.g., stroke, small vessel disease, vascular dementia), less was known about the impact of arterial elasticity on the volume of specific brain regions in relatively healthy individuals such as those included in this study (Hughes et al., 2015; Mattace-Raso et al., 2006; Power et al., 2011; Tanaka et al., 2000; van Sloten et al., 2015a; van Sloten et al., 2015b). These findings are consistent with the regionally specific association between cerebral blood flow (indexed using ASL) and anatomy found in older adults in one of our previous studies (Zimmerman et al., 2014). In that study, localized cerebral blood flow was predictive of specific volumetric measures within the superior frontal and inferior parietal cortex. This phenomenon was local, in the sense that each region’s blood flow was better correlated with each region’s volume than with the volume of the other region. It is possible that these measures of cerebral blood flow were indirectly related to the stiffness of arterial beds within those regions, a relationship that is yet to be investigated.

An alternative possibility for the arterial stiffness/cortical volume relationship is that cortical volumetric reduction is in fact the primary phenomenon: Decline in the capillary bed might lead to increased peripheral resistance, with the development of arterial stiffness being a long-term consequence of this process. If both phenomena were found to exist, they could also lead to a positive feedback, which may amplify their relationships with age. A similar mechanism that may generate a positive feedback is the age-related accumulation of amyloid

beta around the walls of blood vessels, a phenomenon associated with cerebral amyloid angiopathy (Biffi & Greenberg, 2011).

The spatial association between arterial elasticity and cortical volume, emerging with age, provides an important link (albeit only correlational in nature) between these variables, to be further explored in future studies. Specifically, it can be interpreted as suggesting that different individuals present different spatial patterns of cerebrovascular stiffness, and consequently show specific spatial patterns of brain atrophy (or, in fact, vice versa). This may have important practical consequences for the specific patterns of cognitive impairments that these individuals might suffer from. However, it should be noted that this was only an initial study of this relationship, based on a cross-sectional sample, with a relatively small sample size and only investigating healthy individuals. Future studies using longitudinal designs, larger sample sizes, and considering individuals at risk for cerebrovascular problems (e.g. individuals with hypertension, diabetes, high cholesterol levels, etc.) may further validate this approach for characterizing the influence of cerebrovascular factors on cognitive aging. This would also facilitate a detailed examination of possible regional differences in sensitivity to vascular issues, hinted by the results presented in Figure 3. In addition, the relationship between the anatomical brain effects associated with cerebrovascular health (or lack thereof) and cognitive function needs to be clarified further. For instance, individuals could be selected on the basis of particular patterns of arterial dysfunction, and compared in terms of consequent patterns of cognitive dysfunction (or vice versa).

Although this study was planned to specifically explore the *regional* relationships between volumetric and PReFx measures (which were supported by previous reports at the global level, see Fabiani et al., 2014; Tan et al., 2017), we also explored the relationship between arterial elasticity and cortical thickness. In general, thickness estimates showed less powerful associations with PReFx than volume, both for the between- and the within-subject analyses. This result may be due to the lower reliability of the thickness relative to the volume estimates (see Iscan et al., 2015), compounded by the relatively small sample size of the current study (N=47). Further investigations based on a larger sample could determine whether the weaker relationship between arterial elasticity and cortical thickness (relative to volume) is in fact due to lack of sufficient statistical power.

4.3 Specificity to older adults

Although significant overall, the regional intra-individual association between arterial elasticity and anatomy was driven primarily by adults over the age of 48 (Figure 5a). The exact reason for this pattern is unknown, but a number of potential explanations are possible. For example, younger adults experience little atrophy, and therefore less variance exists across regions, leading to a floor effect (see top of figure 6a; see also Beauchet et al., 2013; Fjell et al., 2013; Jochemsen et al., 2015; Rabkin, 2012; Raz et al., 2008; Tsao et al., 2016). Additionally, younger adults also experience less vascular damage from reactive oxidative species, and have more robust compensatory and/or repair mechanisms to mitigate cerebrovascular stiffness effects (El-Assar et al., 2012; Hoenig et al., 2008). This increased

protection might lead to decreased atrophy and a diminished spatial relationship between arterial stiffness and atrophy.

Alternatively, it is also possible that the effects of decreased elasticity, and the accompanying sub-clinical hypoperfusion, might take an extended period of time to significantly impact the gross anatomical size of brain tissue. In this light, a number of studies have suggested a similar time lag as midlife blood pressure has been linked to atrophy later in life (Debette et al., 2011; Korf et al., 2004; Launer et al., 1995; Petrovitch et al., 2000; Swan et al., 1998). Finally, older adults might be more sensitive to subclinical neurovascular stiffening due to other physiological processes that co-occur with advancing age. For instance, aging is also associated with declines in dendritic spine density, myelination, glial alterations, amyloid-β deposition and changes to white matter integrity (Jagust, 2016; Madden et al., 2012; Pannese, 2012; van der Zee, 2015; Wang & Young, 2014). Thus, alterations of arterial elasticity in older individuals might interact with (or summate to) these neurophysiological changes, leading to the regionally specific spatial relationship found in older adults.

Theoretically, the spatial relationship between arterial health and brain volume could also help explain variance in the pattern of cognitive decline observed within an aging individual. Although the current study does not address this issue, previous studies suggest that this might be the case (Wilson et al., 2002; Fabiani et al., 2014; Tan et al., 2017). Previous research has also shown a link between local cortical atrophy and specific changes in cognitive outcomes (Aguilar et al., 2014; Draganski et al., 2013; Hedden & Gabrieli, 2004; Hedden et al., 2014; Kaup et al., 2011; Raz et al., 1998; Raz & Rodrigue, 2006; Rodrigue & Raz, 2004; Salthouse, 2011). This indicates the need for future studies investigating whether the regional associations between cortical atrophy and arterial stiffness may, in turn, lead to declines in the specific cognitive domains supported by the affected regions (see also Steffener et al., 2013; Zimmerman et al., 2014, for similar approaches).

4.5 Limitations

Although the analyses presented here open new possibilities for non-invasive regional measures of cerebrovascular elasticity, a number of limitations exist. The main limitation of optical tomography is its shallow depth sensitivity (≈ 30 mm from the scalp in adults). Although this limitation prevents us from measuring the stiffness of arteries feeding subcortical structures, our depth sensitivity is sufficient for studying the arterial status of the outer cortical mantle (Figure 1a).

Second, due to the cross-sectional nature of our study design, we cannot make direct claims of causality between vascular health and regionally specific neuroanatomical decline. Although establishing such a causal relationship may be difficult, longitudinal studies may help address this issue, at least in terms of determining whether age-related changes in arterial stiffness pre-date or follow cortical volumetric changes.

Third, it could be argued that, although the spatial relationship between arterial elasticity and cortical volume was significant overall and greater for older adults, the effect size of this relationship is relatively small. Specifically, even restricting our analysis to older adults, PReFx explained ≈2% of the volumetric intra-regional variance. However, it is very difficult

to precisely estimate the variance attributable to different factors in cross-sectional studies such as this. For example, here we would expect that most of the variance across regions would actually be due to genetic, maturational, and other factors unrelated to arterial health (e.g., size of brain areas at birth). Future longitudinal studies controlling for these individual factors will help quantify more precisely the effects of arterial health on brain anatomy.

4.6 Conclusion

In summary, the data reported in this paper demonstrate that elasticity, as measured by PReFx obtained with optical tomography (pulse-DOT), can help explain some of the anatomical variance found in healthy participants across the lifespan. These findings were most evident in adults over the age of 48, and may provide insight into sub-clinical phenomenon previously unrecognized through other methodologies. Further validation of these methods in groups with specific cerebrovascular pathologies may lead to a better understanding of the relationship between arterial health, brain anatomy, and brain and cognitive function. For instance, it may be possible that regional measures of arterial elasticity may help predict which individuals and/or brain regions might be most vulnerable to neurovascular insults such as stroke, transient ischemic attacks, white matter hyperintensities, small vessel disease, and vascular dementia.

Acknowledgments

This work was supported by NIH grant 1R56MH097973-01 to G. Gratton and M. Fabiani and by NCRR grant S10-RR029294 to G. Gratton.

References

Aaslid, R. Transcranial Doppler sonography. New York: Springer Science & Business Media; 2012. p. 178

Aguilar C, Muehlboeck JS, Mecocci P, Vellas B, Tsolaki M, Kloszewska I, Soininen H, Lovestone S, Wahlund LO, Simmons A, Westman E, for the AddNeuroMed C. Application of a MRI based index to longitudinal atrophy change in Alzheimer disease, mild cognitive impairment and healthy older individuals in the AddNeuroMed cohort. Frontiers in Aging Neuroscience. 2014; 6:145. [PubMed: 25071554]

Alexander-Bloch A, Giedd JN, Bullmore E. Imaging structural co-variance between human brain regions. Nature reviews Neuroscience. 2013; 14:322–336. [PubMed: 23531697]

Alexander GE, Ryan L, Bowers D, Foster TC, Bizon JL, Geldmacher DS, Glisky EL. Characterizing cognitive aging in humans with links to animal models. Front Aging Neurosci. 2012; 4:21. [PubMed: 22988439]

Alian, AA., Shelley, KH. Photoplethysmography: Analysis of the pulse oximeter waveform. In: Ehrenfeld, MJ., Cannesson, M., editors. Monitoring Technologies in Acute Care Environments: A Comprehensive Guide to Patient Monitoring Technology. New York, NY: Springer New York; 2014. p. 165-178.

Allen J. Photoplethysmography and its application in clinical physiological measurement. Physiological measurement. 2007; 28:R1. [PubMed: 17322588]

Andrews-Hanna JR, Snyder AZ, Vincent JL, Lustig C, Head D, Raichle Marcus E, Buckner RL. Disruption of large-scale brain systems in advanced aging. Neuron. 2007; 56(5):924–935. [PubMed: 18054866]

Beauchet O, Celle S, Roche F, Bartha R, Montero-Odasso M, Allali G, Annweiler C. Blood pressure levels and brain volume reduction: a systematic review and meta-analysis. Journal of Hypertension. 2013; 31:1502–1516. [PubMed: 23811995]

Beck, AT., Steer, RA. Psychological Corporation. San Antonio, TX: 1987. BDI, Beck depression inventory: manual; p. 1-16.

Biffi A, Greenberg SM. Cerebral amyloid angiopathy: A systematic review. J Clin Neurol. 2011; 7:1–9. [PubMed: 21519520]

Blair GW, Doubal FN, Thrippleton MJ, Marshall I, Wardlaw JM. Magnetic resonance imaging for assessment of cerebrovascular reactivity in cerebral small vessel disease: A systematic review. Journal of Cerebral Blood Flow & Metabolism. 2016; 36:833–841. [PubMed: 26884471]

Cabeza R. Hemispheric asymmetry reduction in older adults: the HAROLD model. Psychol Aging. 2002; 17:85–100. [PubMed: 11931290]

Cannesson M, Le Manach Y, Hofer CK, Goarin JP, Lehot JJ, Vallet B, Tavernier B. Assessing the diagnostic accuracy of pulse pressure variations for the prediction of fluid responsiveness. A “Gray Zone” approach. The Journal of the American Society of Anesthesiologists. 2011; 115:231–241.

Casserly I, Topol EJ. Convergence of atherosclerosis and Alzheimer’s disease: inflammation, cholesterol, and misfolded proteins. The Lancet. 2004; 363:1139–1146.

Chiarelli AM, Maclin EL, Fabiani M, Gratton G. A kurtosis-based wavelet algorithm for motion artifact correction of fNIRS data. NeuroImage. 2015a; 112:128–137. [PubMed: 25747916]

Chiarelli AM, Maclin EL, Low KA, Fabiani M, Gratton G. Comparison of procedures for co-registering scalp-recording locations to anatomical magnetic resonance images. Journal of biomedical optics. 2015b; 20:016009–016009. [PubMed: 25574993]

Chiarelli AM, Maclin EL, Low KA, Mathewson KE, Fabiani M, Gratton G. Combining energy and Laplacian regularization to accurately retrieve the depth of brain activity of diffuse optical tomographic data. Journal of Biomedical Optics. 2016; 21(3):036008–036008.

Cook LB. Extracting arterial flow waveforms from pulse oximeter waveforms. Anaesthesia. 2001; 56:551–555. [PubMed: 11412161]

Corpet F. Multiple sequence alignment with hierarchical clustering. Nucleic Acids Research. 1988; 16:10881–10890. [PubMed: 2849754]

Dale AM, Fischl B, Sereno MI. Cortical surface-based analysis. I. Segmentation and surface reconstruction. Neuroimage. 1999; 9:179–94. [PubMed: 9931268]

Debette S, Seshadri S, Beiser A, Au R, Himali JJ, Palumbo C, Wolf PA, DeCarli C. Midlife vascular risk factor exposure accelerates structural brain aging and cognitive decline. Neurology. 2011; 77:461–468. [PubMed: 21810696]

Dehghani H, Eames ME, Yalavarthy PK, Davis SC, Srinivasan S, Carpenter CM, Pogue BW, Paulsen KD. Near infrared optical tomography using NIRFAST: Algorithm for numerical model and image reconstruction. Communications in Numerical Methods in Engineering. 2009; 25:711–732.

Desikan RS, Segonne F, Fischl B, Quinn BT, Dickerson BC, Blacker D, Buckner RL, Dale AM, Maguire RP, Hyman BT, Albert MS, Killiany RJ. An automated labeling system for subdividing the human cerebral cortex on MRI scans into gyral based regions of interest. Neuroimage. 2006; 31:968–980. [PubMed: 16530430]

Draganski B, Lutti A, Kherif F. Impact of brain aging and neurodegeneration on cognition: evidence from MRI. Current opinion in neurology. 2013; 26:640–645. [PubMed: 24184970]

Eggebrecht AT, Ferradal SL, Robichaux-Viehoever A, Hassanpour MS, Dehghani H, Snyder AZ, Hershey T, Culver JP. Mapping distributed brain function and networks with diffuse optical tomography. Nature photonics. 2014; 8:448–454. [PubMed: 25083161]

El-Assar M, Angulo J, Vallejo S, Peiró C, Sánchez-Ferrer CF, Rodríguez-Mañas L. Mechanisms involved in the aging-induced vascular dysfunction. Frontiers in physiology. 2012; 3:132. [PubMed: 22783194]

Erickson KI, Hillman CH, Kramer AF. Physical activity, brain, and cognition. Current Opinion in Behavioral Sciences. 2015; 4:27–32.

Fabiani M. It was the best of times, it was the worst of times: a psychophysiologist’s view of cognitive aging. Psychophysiology. 2012; 49:283–304. [PubMed: 22220910]

Fabiani M, Gratton G. Aging, working memory, and attention control: a tale of two processing streams?. Front. Hum. Neurosci. Conference Abstract: XI International Conference on Cognitive Neuroscience (ICON XI). 2012

Fabiani M, Low KA, Tan CH, Zimmerman B, Fletcher MA, Schneider-Garces N, Maclin EL, Chiarelli AM, Sutton BP, Gratton G. Taking the pulse of aging: Mapping pulse pressure and elasticity in cerebral arteries with optical methods. Psychophysiology. 2014; 51:1072–1088. [PubMed: 25100639]

Fang Q, Boas DA. Tetrahedral mesh generation from volumetric binary and grayscale images). Biomedical Imaging: From Nano to Macro. 2009:1142–1145. ISBI'09. IEEE International Symposium on.

Fischl B, Dale AM. Measuring the thickness of the human cerebral cortex from magnetic resonance images. Proc Natl Acad Sci U S A. 2000; 97:11050–5. [PubMed: 10984517]

Fischl B, Liu A, Dale AM. Automated manifold surgery: constructing geometrically accurate and topologically correct models of the human cerebral cortex. IEEE transactions on medical imaging. 2001; 20:70–80. [PubMed: 11293693]

Fischl B, Sereno MI, Dale AM. Cortical surface-based analysis. II: Inflation, flattening, and a surface-based coordinate system. Neuroimage. 1999a; 9:195–207. [PubMed: 9931269]

Fischl B, Sereno MI, Tootell RB, Dale AM. High-resolution intersubject averaging and a coordinate system for the cortical surface. Hum Brain Mapp. 1999b; 8:272–84. [PubMed: 10619420]

Fischl B, van der Kouwe A, Destrieux C, Halgren E, Ségonne F, Salat DH, Busa E, Seidman LJ, Goldstein J, Kennedy D, Caviness V, Makris N, Rosen B, Dale AM. Automatically Parcellating the Human Cerebral Cortex. Cerebral Cortex. 2004; 14:11–22. [PubMed: 14654453]

Fletcher MA, Low KA, Boyd R, Zimmermam B, Gordon BA, Tan CH, Schneider-Garces N, Sutton BP, Gratton G, Fabiani M. Comparing fitness and aging effects on brain anatomy. Frontiers in Human Neuroscience. 2016; 10:286. [PubMed: 27445740]

Fjell AM, Westlye LT, Grydeland H, Amlien I, Espeseth T, Reinvang I, Raz N, Holland D, Dale AM, Walhovd KB, Alzheimer Disease Neuroimaging I. Critical ages in the life course of the adult brain: nonlinear subcortical aging. Neurobiol Aging. 2013; 34:2239–47. [PubMed: 23643484]

Friston KJ, Holmes AP, Worsley KJ, Poline JP, Frith CD, Frackowiak RSJ. Statistical parametric maps in functional imaging: A general linear approach. Human Brain Mapping. 1994; 2:189–210.

Gómez-Pinilla F. Brain foods: the effects of nutrients on brain function. Nature reviews. Neuroscience. 2008; 9:568–578. [PubMed: 18568016]

Gordon BA, Rykhlevskaia EI, Brumback CR, Lee Y, Elavsky S, Konopack JF, McAuley E, Kramer AF, Colcombe S, Gratton G, Fabiani M. Neuroanatomical correlates of aging, cardiopulmonary fitness level, and education. Psychophysiology. 2008; 45:825–38. [PubMed: 18627534]

Gratton G, Corballis PM. Removing the heart from the brain: Compensation for the pulse artifact in the photon migration signal. Psychophysiology. 1995; 32:292–299. [PubMed: 7784538]

Hatanaka R, Obara T, Watabe D, Ishikawa T, Kondo T, Ishikura K, Aikawa T, Aono Y, Hara A, Metoki H, Asayama K, Kikuya M, Mano N, Ohkubo T, Izumi SI, Imai Y. Association of arterial stiffness with silent cerebrovascular lesions: The Ohasama study. Cerebrovascular Diseases. 2011; 31:329–337. [PubMed: 21212664]

Hayes, AF. Introduction to mediation, moderation, and conditional process analysis: A regression-based approach. New York, NY: Guilford Press; 2008.

Hedden T, Gabrieli JDE. Insights into the ageing mind: A view from cognitive neuroscience. Nature Reviews Neuroscience. 2004; 5:87–U12. [PubMed: 14735112]

Hedden T, Schultz AP, Rieckmann A, Mormino EC, Johnson KA, Sperling RA, Buckner RL. Multiple brain markers are linked to age-related variation in cognition. Cerebral Cortex. 2014; 26:1388–1400. [PubMed: 25316342]

Hoenig MR, Bianchi C, Rosenzweig A, Sellke FW. Decreased vascular repair and neovascularization with ageing: mechanisms and clinical relevance with an emphasis on hypoxia-inducible factor-1. Current molecular medicine. 2008; 8:754–767. [PubMed: 19075673]

Hohman TJ, Bell SP, Jefferson AL, for the Alzheimer's Disease Neuroimaging, I. The role of vascular endothelial growth factor in neurodegeneration and cognitive decline: Exploring interactions with biomarkers of alzheimer disease. JAMA Neurology. 2015; 72:520–529. [PubMed: 25751166]

Hoshi Y, Tamura M. Detection of dynamic changes in cerebral oxygenation coupled to neuronal function during mental work in man. Neuroscience Letters. 1993; 150:5–8. [PubMed: 8469403]

Hughes TM, Craft S, Lopez OL. Review of 'the potential role of arterial stiffness in the pathogenesis of Alzheimer's disease'. Neurodegenerative Disease Management. 2015; 5:121–135. [PubMed: 25894876]

Iscan Z, Jin TB, Kendrick A, Szeglin B, Lu H, Trivedi M, Fava M, McGrath PJ, Weissman M, Kurian BT, Adams P. Test–retest reliability of FreeSurfer measurements within and between sites: effects of visual approval process. Human brain mapping. 2015; 36:3472–3485. [PubMed: 26033168]

Ishimaru A. Diffusion of light in turbid material. Appl Opt. 1989; 28:2210–2215. [PubMed: 20555501]

Izzo JL Jr, Shykoff BE. Arterial stiffness: clinical relevance, measurement, and treatment. Rev Cardiovasc Med. 2001; 2:29–40. [PubMed: 12478235]

Jack CR Jr, Twomey CK, Zinsmeister AR, Sharbrough FW, Petersen RC, Cascino GD. Anterior temporal lobes and hippocampal formations: normative volumetric measurements from MR images in young adults. Radiology. 1989; 172:549–54. [PubMed: 2748838]

Jagust W. Is amyloid-β harmful to the brain? Insights from human imaging studies. Brain. 2016; 139(Pt 1):23–30. [PubMed: 26614753]

Jochemsen HM, Muller M, Bots ML, Scheltens P, Vincken KL, Mali WPTM, van der Graaf Y, Geerlings MI. Arterial stiffness and progression of structural brain changes: The SMART-MR study. Neurology. 2015; 84:448–455. [PubMed: 25552578]

Jolly TA, Cooper PS, Badwi SA, Phillips NA, Rennie JL, Levi CR, Drysdale KA, Parsons MW, Michie PT, Karayanidis F. Microstructural white matter changes mediate age-related cognitive decline on the Montreal Cognitive Assessment (MoCA). Psychophysiology. 2016; 53(2):258–67. DOI: 10.1111/psyp.12565 [PubMed: 26511789]

Jolly TA, Cooper PS, Rennie JL, Levi CR, Lenroot R, Parsons MW, Michie PT, Karayanidis F. Age-related decline in task switching is linked to both global and tract-specific changes in white matter microstructure. Human Brain Mapping. 2017; 38(3):1588–1603. DOI: 10.1002/hbm.23473 [PubMed: 27879030]

Kalaria RN, Akinyemi R, Ihara M. Does vascular pathology contribute to Alzheimer changes? Journal of the Neurological Sciences. 2012; 322:141–147. [PubMed: 22884479]

Kaup AR, Mirzakhanian H, Jeste DV, Eyler LT. A review of the brain structure correlates of successful cognitive aging. The Journal of neuropsychiatry and clinical neurosciences. 2011; 23:6–15. [PubMed: 21304134]

Korf ESC, White LR, Scheltens P, Launer LJ. Midlife blood pressure and the risk of hippocampal atrophy: The Honolulu Asia aging study. Hypertension. 2004; 44:29–34. [PubMed: 15159381]

Kramer AF, Colcombe SJ, McAuley E, Scalf PE, Erickson KI. Fitness, aging and neurocognitive function. Neurobiol Aging. 2005; 26(1):124–127. [PubMed: 16213062]

Kramer AF, Erickson KI, Colcombe SJ. Exercise, cognition, and the aging brain. J Appl Physiol (1985). 2006; 101:1237–42. [PubMed: 16778001]

Launer LJ, Masaki K, Petrovitch H, Foley D, Havlik RJ. The association between midlife blood pressure levels and late-life cognitive function: The honolulu-asia aging study. JAMA. 1995; 274:1846–1851. [PubMed: 7500533]

Madden DJ, Bennett IJ, Burzynska A, Potter GG, Chen N-k, Song AW. Diffusion tensor imaging of cerebral white matter integrity in cognitive aging. Biochimica et Biophysica Acta (BBA) - Molecular Basis of Disease. 2012; 1822:386–400. [PubMed: 21871957]

Mattace-Raso FUS, van der Cammen TJM, Hofman A, van Popele NM, Bos ML, Schalekamp MADH, Asmar R, Reneman RS, Hoeks APG, Breteler MMB, Witteman JCM. Arterial stiffness and risk of coronary heart disease and stroke: The Rotterdam Study. Circulation. 2006; 113:657–663. [PubMed: 16461838]

Mayeux R, Stern Y, Rosen J, Leventhal J. Depression, intellectual impairment, and Parkinson disease. Neurology. 1981; 31:645–50. [PubMed: 7195481]

Monti JM, Moulton CJ, Cohen NJ. The role of nutrition on cognition and brain health in ageing: a targeted approach. Nutrition Research Reviews. 2015; 28:167–180. [PubMed: 26650244]

Murkin JM, Arango M. Near-infrared spectroscopy as an index of brain and tissue oxygenation. British Journal of Anaesthesia. 2009; 103:i3–i13. [PubMed: 20007987]

Oldfield RC. The assessment and analysis of handedness: The Edinburgh inventory. Neuropsychologia. 1971; 9:97–113. [PubMed: 5146491]

Oliver JJ, Webb DJ. Noninvasive assessment of arterial stiffness and risk of atherosclerotic events. Arteriosclerosis, thrombosis, and vascular biology. 2003; 23:554–566.

Pannese E. Neuroglial cells: morphological changes during normal aging. Rendiconti Lincei. 2012; 24:101–106.

Park DC, Lautenschlager G, Hedden T, Davidson NS, Smith AD, Smith PK. Models of visuospatial and verbal memory across the adult life span. Psychol Aging. 2002; 17:299–320. [PubMed: 12061414]

Paulsen KD, Jiang H. Spatially varying optical property reconstruction using a finite element diffusion equation approximation. Medical Physics. 1995; 22:691–701. [PubMed: 7565358]

Penny, WD., Friston, KJ., Ashburner, JT., Kiebel, SJ., Nichols, TE. Statistical parametric mapping: the analysis of functional brain images: the analysis of functional brain images. London, UK: Academic press; 2011. p. 679

Peres R, De Guio F, Chabriat H, Jouvent E. Alterations of the cerebral cortex in sporadic small vessel disease: A systematic review of in vivo MRI data. Journal of Cerebral Blood Flow & Metabolism. 2016; 36:681–695. [PubMed: 26787108]

Petrovitch H, White LR, Izmirilian G, Ross GW, Havlik RJ, Markesbery W, Nelson J, Davis DG, Hardman J, Foley DJ, Launer LJ. Midlife blood pressure and neuritic plaques, neurofibrillary tangles, and brain weight at death: the HAAS☆. Neurobiology of Aging. 2000; 21:57–62. [PubMed: 10794849]

Pfefferbaum A, Sullivan EV, Hedehus M, Lim KO, Adalsteinsson E, Moseley M. Age-related decline in brain white matter anisotropy measured with spatially corrected echo-planar diffusion tensor imaging. Magnetic resonance in medicine: official journal of the Society of Magnetic Resonance in Medicine/Society of Magnetic Resonance in Medicine. 2000; 44:259–68.

Power MC, Weuve J, Gagne JJ, McQueen MB, Viswanathan A, Blacker D. The association between blood pressure and incident Alzheimer disease: a systematic review and meta-analysis. Epidemiology (Cambridge, Mass). 2011; 22:646–659.

Rabkin SW. Arterial stiffness: detection and consequences in cognitive impairment and dementia of the elderly. Journal of Alzheimer's Disease. 2012; 32:541–549.

Raz N, Ghisletta P, Rodrigue KM, Kennedy KM, Lindenberger U. Trajectories of brain aging in middle-aged and older adults: regional and individual differences. Neuroimage. 2010; 51:501–11. [PubMed: 20298790]

Raz N, Gunning-Dixon FM, Head D, Dupuis JH, Acker JD. Neuroanatomical correlates of cognitive aging: evidence from structural magnetic resonance imaging. Neuropsychology. 1998; 12:95–114. [PubMed: 9460738]

Raz N, Lindenberger U, Ghisletta P, Rodrigue KM, Kennedy KM, Acker JD. Neuroanatomical correlates of fluid intelligence in healthy adults and persons with vascular risk factors. Cereb Cortex. 2008; 18:718–26. [PubMed: 17615248]

Raz N, Lindenberger U, Rodrigue KM, Kennedy KM, Head D, Williamson A, Dahle C, Gerstorf D, Acker JD. Regional brain changes in aging healthy adults: general trends, individual differences and modifiers. Cereb Cortex. 2005; 15:1676–89. [PubMed: 15703252]

Raz N, Rodrigue KM. Differential aging of the brain: patterns, cognitive correlates and modifiers. Neuroscience and biobehavioral reviews. 2006; 30:730–48. [PubMed: 16919333]

Raz N, Rodrigue KM, Kennedy KM, Acker JD. Vascular health and longitudinal changes in brain and cognition in middle-aged and older adults. Neuropsychology. 2007; 21:149–157. [PubMed: 17402815]

Rodrigue KM, Raz N. Shrinkage of the entorhinal cortex over five years predicts memory performance in healthy adults. The Journal of neuroscience: the official journal of the Society for Neuroscience. 2004; 24:956–63. [PubMed: 14749440]

Salthouse TA. Selective review of cognitive aging. Journal of the International Neuropsychological Society. 2010; 16:754–760. [PubMed: 20673381]

Salthouse TA. Neuroanatomical substrates of age-related cognitive decline. Psychological Bulletin. 2011; 137:753–784. [PubMed: 21463028]

Schaie KW. The Hazards of Cognitive Aging. The Gerontologist. 1989; 29:484–493. [PubMed: 2521108]

Segers P, Rabben SI, De Backer J, De Sutter J, Gillebert TC, Van Bortel L, Verdonck P. Functional analysis of the common carotid artery: relative distension differences over the vessel wall measured in vivo. Journal of Hypertension. 2004; 22:973–981. [PubMed: 15097238]

Shi Y, Thrippleton MJ, Makin SD, Marshall I, Geerlings MI, de Craen AJ, van Buchem MA, Wardlaw JM. Cerebral blood flow in small vessel disease: A systematic review and meta-analysis. Journal of Cerebral Blood Flow & Metabolism. 2016; 36:1653–1667. [PubMed: 27496552]

Singer J, Trollor JN, Baune BT, Sachdev PS, Smith E. Arterial stiffness, the brain and cognition: A systematic review. Ageing Research Reviews. 2014; 15:16–27. [PubMed: 24548924]

Steffener J, Brickman AM, Habeck CG, Salthouse TA, Stern Y. Cerebral blood flow and gray matter volume covariance patterns of cognition in aging. Human Brain Mapping. 2013; 34:3267–3279. [PubMed: 22806997]

Stergiou GS, Lourida P, Tzamouranis D, Baibas NM. Unreliable oscillometric blood pressure measurement: prevalence, repeatability and characteristics of the phenomenon. J Hum Hypertens. 2009; 23:794–800. [PubMed: 19322203]

Swan GE, DeCarli C, Miller BL, Reed T, Wolf PA, Jack LM, Carmelli D. Association of midlife blood pressure to late-life cognitive decline and brain morphology. Neurology. 1998; 51:986–993. [PubMed: 9781518]

Tan CH, Low KA, Schneider-Garces N, Zimmerman B, Fletcher MA, Gratton G, Fabiani M. Optical measures of changes in cerebral vascular tone during voluntary breath holding and a sternberg memory task. Biological Psychology. 2016; 118:184–194. [PubMed: 27235126]

Tan CH, Low KA, Kong T, Fletcher MA, Zimmerman B, Maclin EL, Chiarelli AM, Gratton G, Fabiani M. Mapping cerebral pulse pressure and arterial compliance over the lifespan with optical imaging. PloS One. 2017; 12(2):e0171305.doi: 10.1371/journal.pone.0171305 [PubMed: 28234912]

Tanaka H, Dinenno FA, Monahan KD, Clevenger CM, DeSouza CA, Seals DR. Aging, habitual exercise, and dynamic arterial compliance. Circulation. 2000; 102:1270–1275. [PubMed: 10982542]

Tian F, Liu H. Depth-compensated diffuse optical tomography enhanced by general linear model analysis and an anatomical atlas of human head. NeuroImage. 2014; 85:166–180. [PubMed: 23859922]

Toga AW, Thompson PM. Genetics of brain structure and. Annual Review of Neuroscience. 2005; 28:1–23.

Tsao CW, Himali JJ, Beiser AS, Larson MG, DeCarli C, Vasan RS, Mitchell GF, Seshadri S. Association of arterial stiffness with progression of subclinical brain and cognitive disease. Neurology. 2016; 86:619–626. [PubMed: 26791155]

Unverzagt F, McClure L, Wadley V, Jenny N, Go R, Cushman M, Kissela B, Kelley B, Kennedy R, Moy C. Vascular risk factors and cognitive impairment in a stroke-free cohort. Neurology. 2011; 77:1729–1736. [PubMed: 22067959]

van der Zee EA. Synapses, spines and kinases in mammalian learning and memory, and the impact of aging. Neuroscience & Biobehavioral Reviews. 2015; 50:77–85. [PubMed: 24998408]

van Norden AG, de Laat KF, Gons RA, van Uden IW, van Dijk EJ, van Oudheusden LJ, Esselink RA, Bloem BR, van Engelen BG, Zwarts MJ, Tendolkar I, Olde-Rikkert MG, van der Vlugt MJ, Zwiers MP, Norris DG, de Leeuw FE. Causes and consequences of cerebral small vessel disease. The RUN DMC study: a prospective cohort study. Study rationale and protocol. BMC Neurology. 2011; 11:29. [PubMed: 21356112]

van Sloten TT, Protogerou AD, Henry RMA, Schram MT, Launer LJ, Stehouwer CDA. Association between arterial stiffness, cerebral small vessel disease and cognitive impairment: A systematic review and meta-analysis. Neuroscience & Biobehavioral Reviews. 2015a; 53:121–130. [PubMed: 25827412]

van Sloten TT, Sedaghat S, Laurent S, London GM, Pannier B, Ikram MA, Kavousi M, Mattace-Raso F, Franco OH, Boutouyrie P, Stehouwer CDA. Carotid stiffness is associated with incident stroke.

A systematic review and individual participant data meta-analysis. Journal of the American College of Cardiology. 2015b; 66:2116–2125. [PubMed: 26541923]

Villringer A, Chance B. Non-invasive optical spectroscopy and imaging of human brain function. Trends in Neurosciences. 1997; 20:435–442. [PubMed: 9347608]

Voss MW, Vivar C, Kramer AF, van Praag H. Bridging animal and human models of exercise-induced brain plasticity. Trends in Cognitive Sciences. 2013; 17:525–544. [PubMed: 24029446]

Walhovd KB, Westlye LT, Amlien I, Espeseth T, Reinvang I, Raz N, Agartz I, Salat DH, Greve DN, Fischl B, Dale AM, Fjell AM. Consistent neuroanatomical age-related volume differences across multiple samples. Neurobiology of Aging. 2011; 32:916–932. [PubMed: 19570593]

Wang S, Young KM. White matter plasticity in adulthood. Neuroscience. 2014; 276:148–160. [PubMed: 24161723]

Ward JH. Hierarchical grouping to optimize an objective Function. Journal of the American Statistical Association. 1963; 58:236–244.

Whalen C, Maclin EL, Fabiani M, Gratton G. Validation of a method for coregistering scalp recording locations with 3D structural MR images. Human Brain Mapping. 2008; 29:1288–1301. [PubMed: 17894391]

Wilson RS, Beckett LA, Barnes LL, Schneider JA, Bach J, Evans DA, Bennett DA. Individual differences in rates of change in cognitive abilities of older persons. Psychology and aging. 2002; 17:179. [PubMed: 12061405]

Wisely NA, Cook LB. Arterial flow waveforms from pulse oximetry compared with measured Doppler flow waveforms. Anaesthesia. 2001; 56:556–561. [PubMed: 11412162]

Yan L, Liu CY, Smith RX, Jog M, Langham M, Krasileva K, Chen Y, Ringman JM, Wang DJJ. Assessing intracranial vascular compliance using dynamic arterial spin labeling. NeuroImage. 2016; 124:433–441. [PubMed: 26364865]

Zimmerman B, Sutton BP, Low KA, Fletcher MA, Tan CH, Schneider-Garces N, Li Y, Ouyang C, Maclin EL, Gratton G, Fabiani M. Cardiorespiratory fitness mediates the effects of aging on cerebral blood flow. Frontiers in Aging Neuroscience. 2014; 6:59. [PubMed: 24778617]

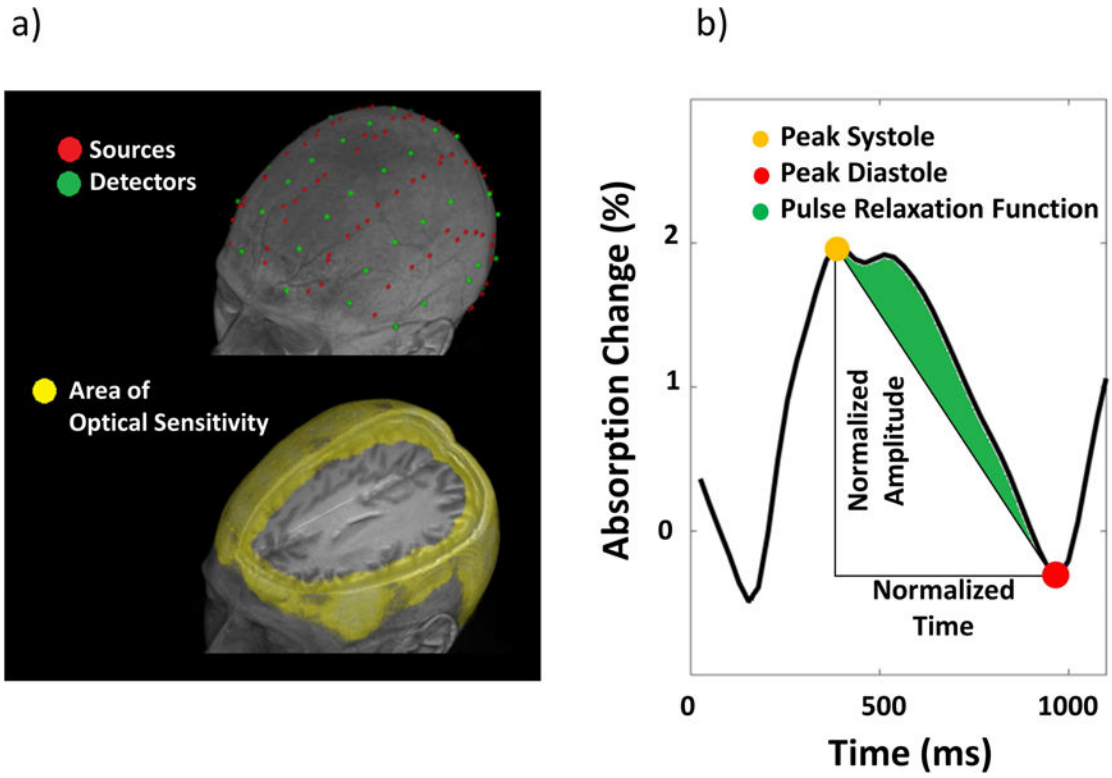

Figure 1.

(a) Optode montage (top) and sensitivity map (bottom) rendered onto the structural MRI image of the same representative participant. The optode montage allowed for the investigation of cortical regions up to a depth of ~30 mm. In the average optical sensitivity map (Jacobian), shown in yellow are points with sensitivity <1/1000 of the maximum sensitivity (b) Schematic diagram describing the estimation of pulse relaxation function (PReFx) for a particular pulse shape. PReFx (green area) is defined as the difference between the observed area under the pulse (normalized by the peak-to-peak systole-diastole amplitude and by the interbeat interval) and the area that would reflect a linear relaxation of the arteries across the interval between the systolic and the diastolic peaks. PReFx is a measure of an area; however, since both the vertical and horizontal axes are normalized, it is essentially dimensionless, with a range between −5 and +.5.

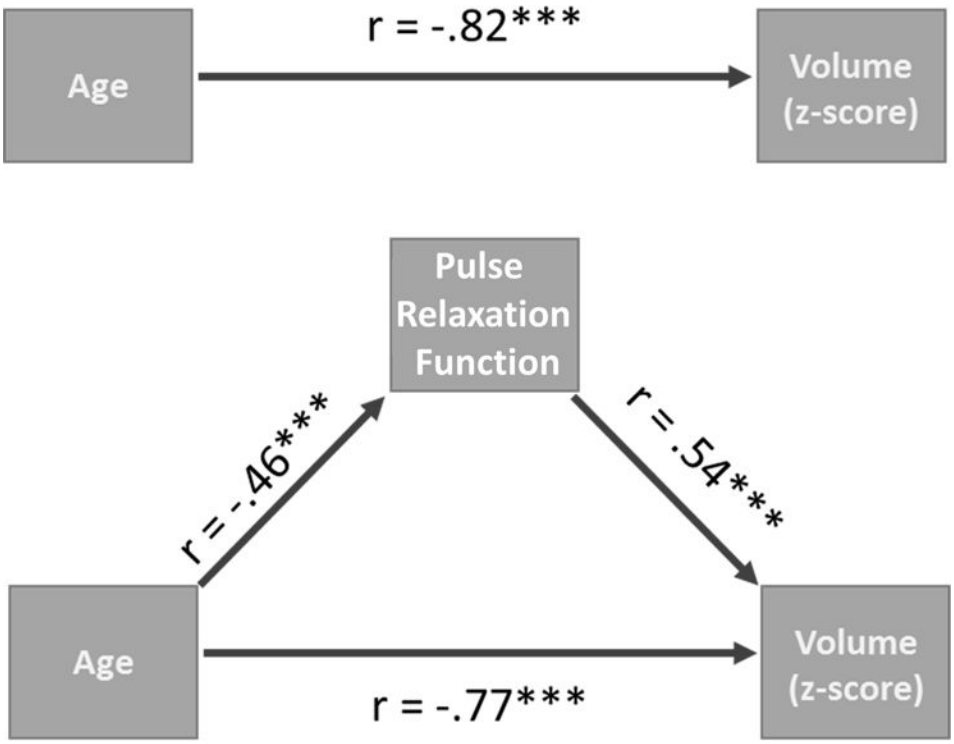

Figure 2.

Schematic representations of the path diagram for the mediation effect of global arterial elasticity (PReFx) on the association between age and global brain volume. (a) Correlation between age and global volume before the mediation analysis. (b) Correlation between age and global PReFx. (c) Correlation between global PReFx and global volume. (d) Correlation between age and global volume after partialing out the effects of global PReFx. The critical comparison is between (a) and (d): The association between PReFx and global brain volume was significantly reduced (bootstrap's $p<.05$) when the mediating effects of arterial elasticity were partialed out.

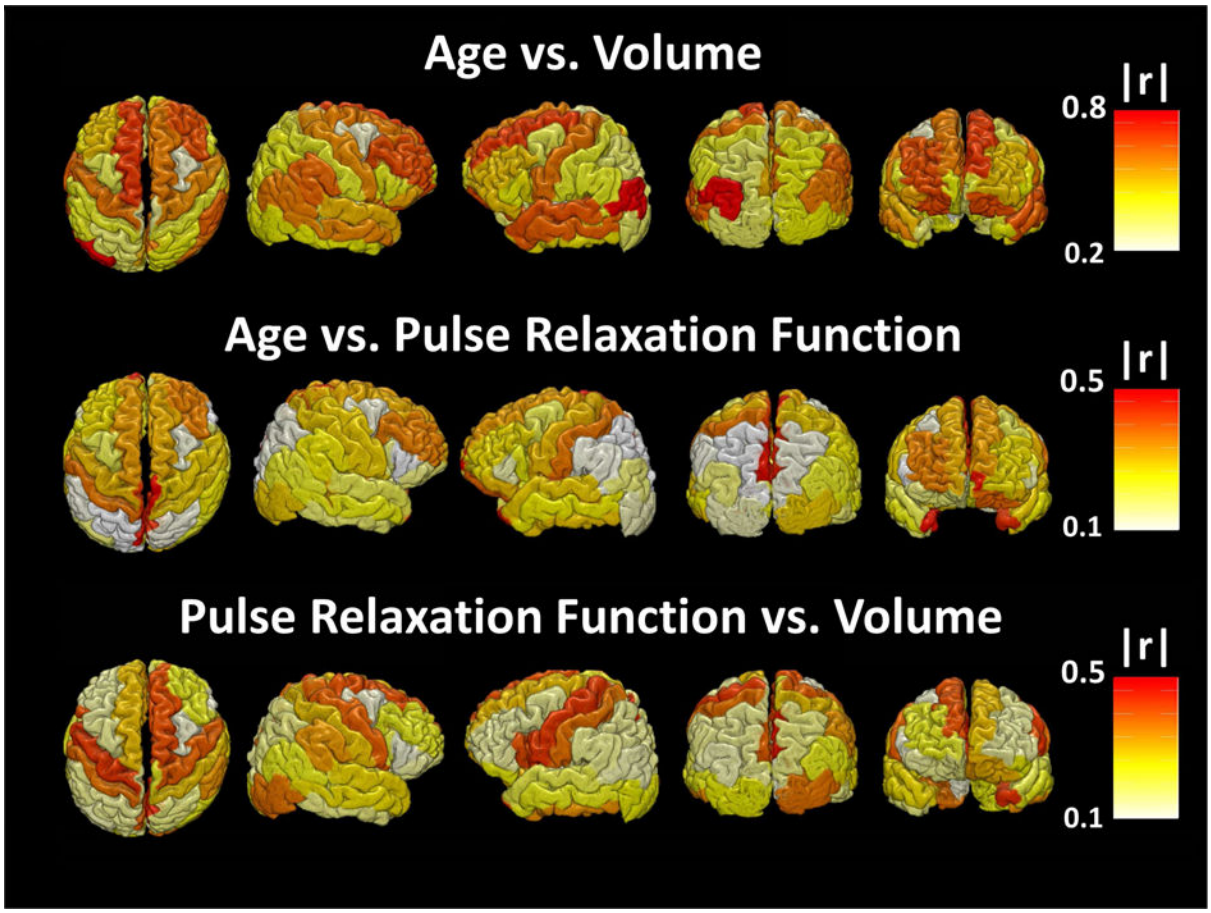

Figure 3.

Maps depicting the unsigned correlations (computed across the entire sample of 47 subjects) between age, volume and the pulse relaxation function (PReFx) for the 50 Freesurfer ROIs. Colors represent the size of the correlations (see scales shown on the right). (Top) Correlations between age and cortical volume; (Middle) correlations between age and PReFx; and (Bottom) correlations between PReFx and cortical volume. The correlations between age and volume and age and PReFx were always negative, whereas the correlations between volume and PReFx were always positive for each ROI examined.

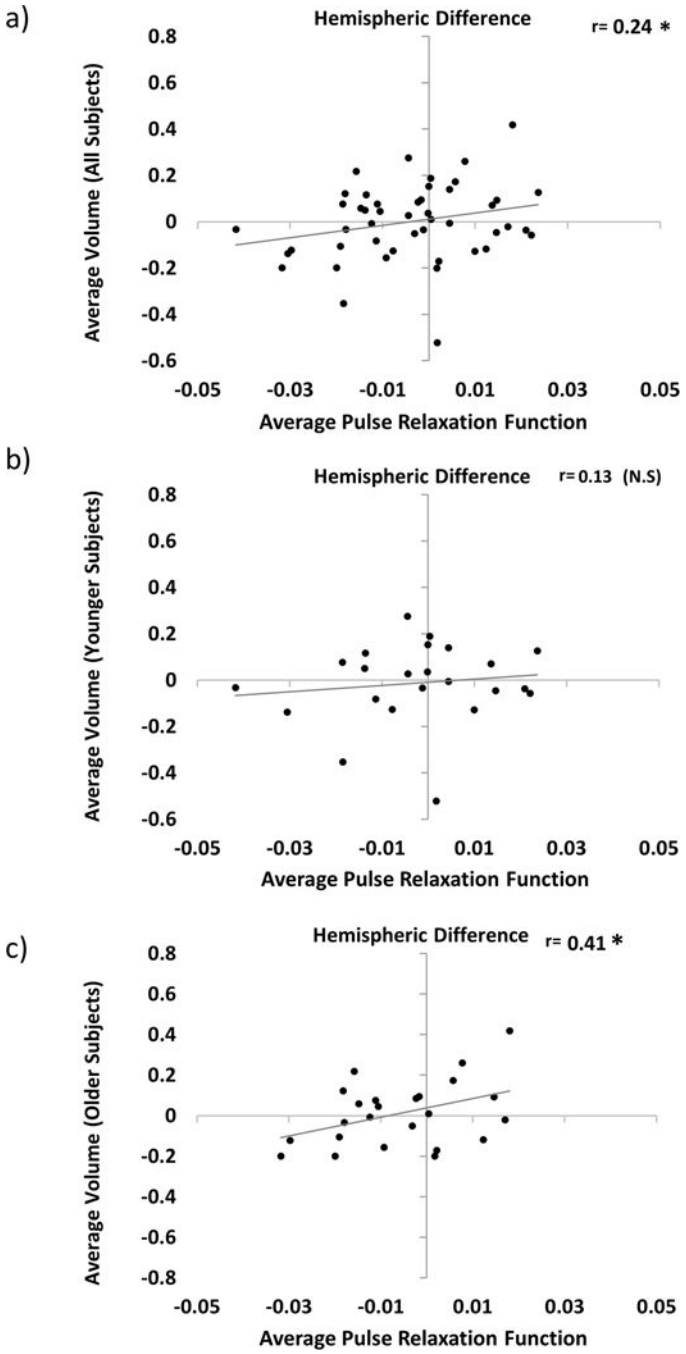

Figure 4.

Scatter plots depicting the relationship between hemispheric differences in average cortical volume (Right Hemisphere – Left Hemisphere) and average PReFx (Right Hemisphere – Left Hemisphere) for all participants (a); and for those younger (b) and older (c) than age 48 (i.e., based on a median split by age). +p<.10, *p<.05, **p<.01, ***p<.001 (one-tailed).

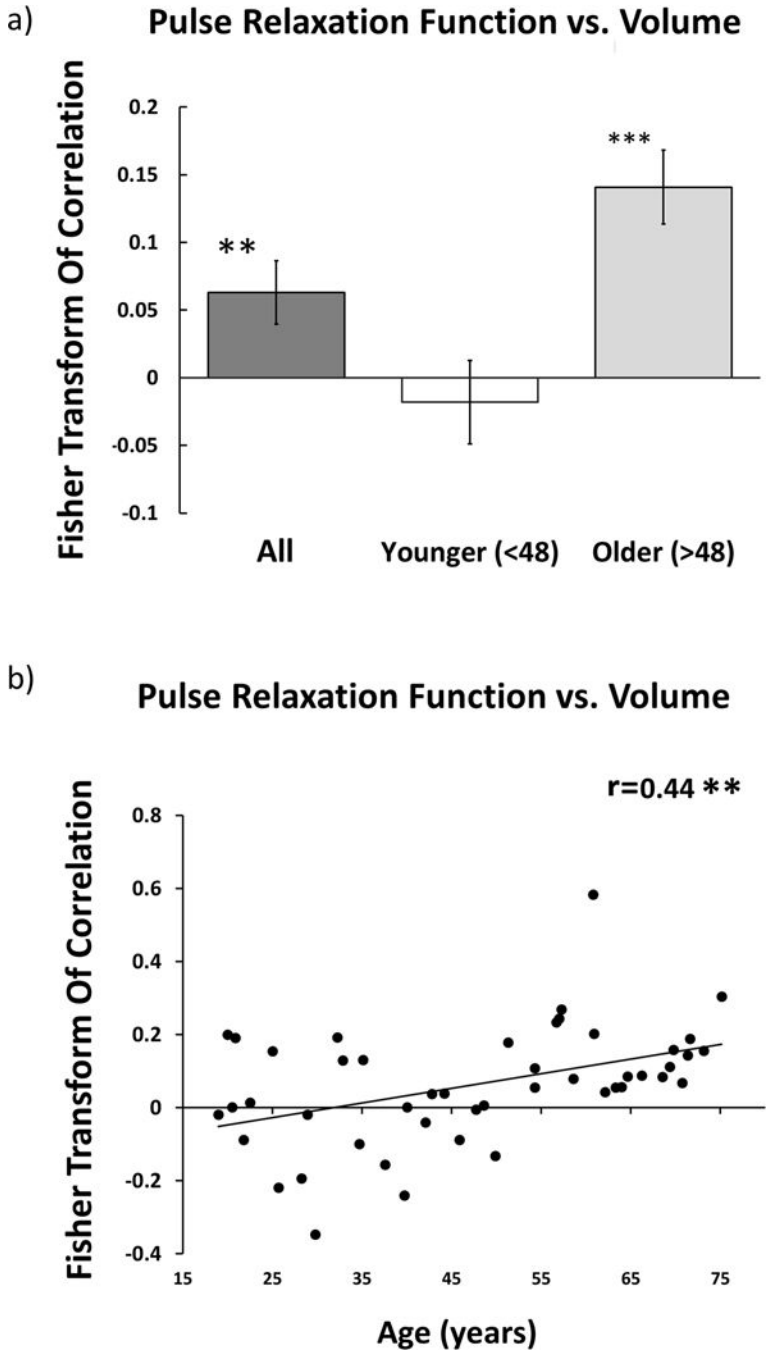

Figure 5.

(a) Histogram of the average spatial association within participants for all participants (dark grey box), and separately for those younger (white box) and older (light-gray box) than age 48. Error bars represent the standard error of the mean. (b) Scatter plots depicting the relationship between age and the Fisher-Transform of the intra-participant correlation between regional anatomy and regional PReFx. Each dot represents the Fisher-transformed correlation for a different individual.

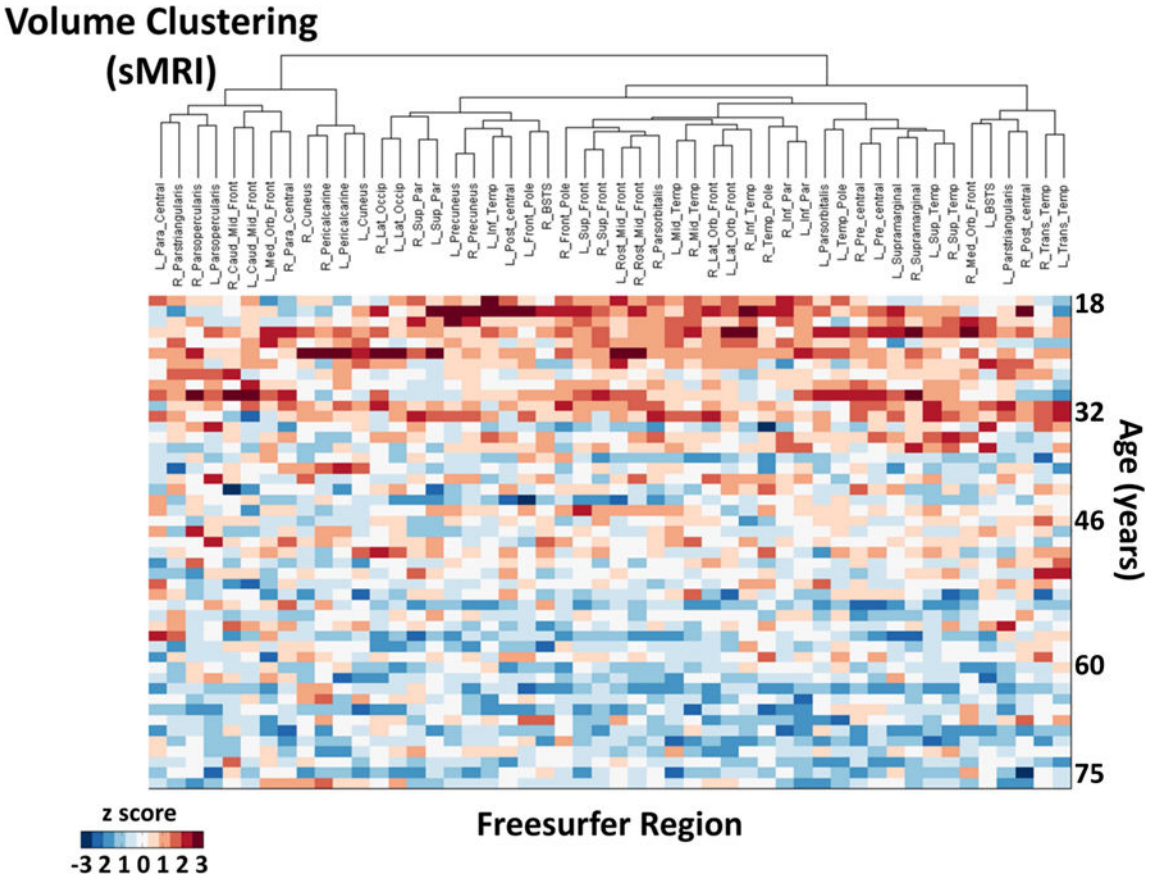

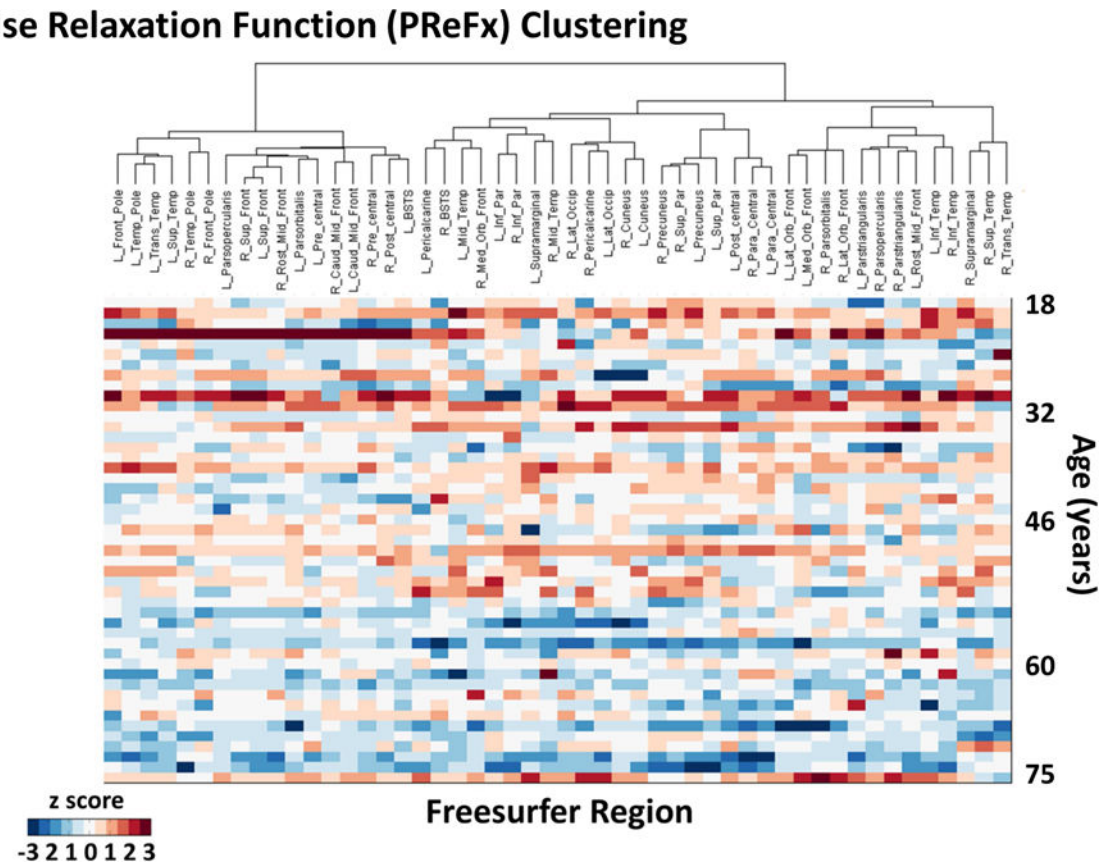

Figure 6.

Spatial dendrograms and data matrices for the hierarchical cluster analysis, with rows (each representing a subject) ordered by age (in years) from youngest (top) to oldest (bottom) and columns representing the 50 ROIs (ordered according to their clustering). The heights of the dendrogram branches represent the distances (based on the metric employed) between the different regions/clusters. (a) Volumetric clusters (color scale indicates volumetric *z* scores for each subject and region); (b) PReFx clusters (color scale indicates PReFx *z* scores for each subject and region). Note that for both (a) and (b) higher *z* scores (reds) tend to appear in the upper sections of the matrices (younger subjects), and smaller z scores (blues) tend to appear in the lower sections (older adults), although within-subject (i.e., within row) variability is also apparent.

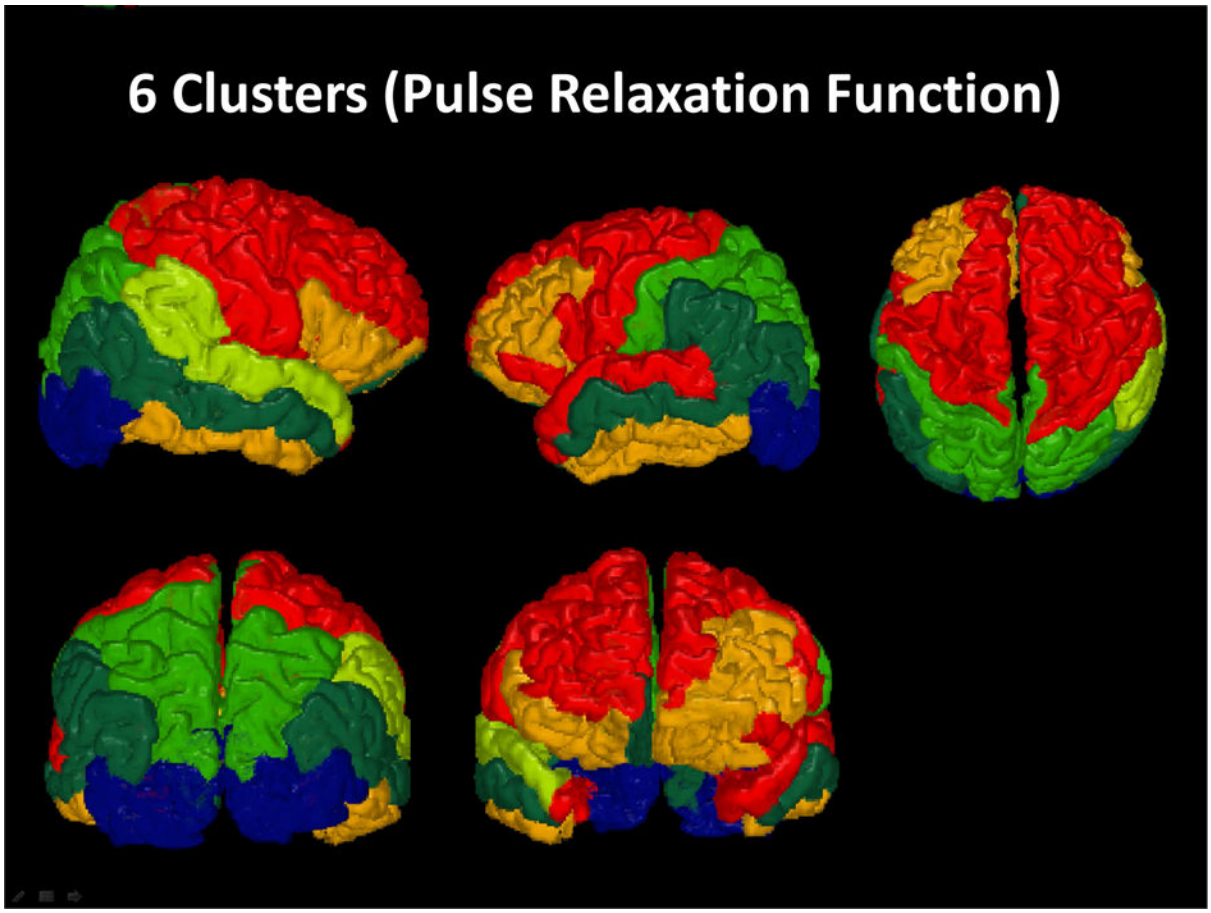

Figure 7.

3-D rendered maps based on an analysis grouping the 50 original ROIs into 6-clusters using a hierarchical agglomerative approach applied to PReFx data. Colors denote the different clusters.

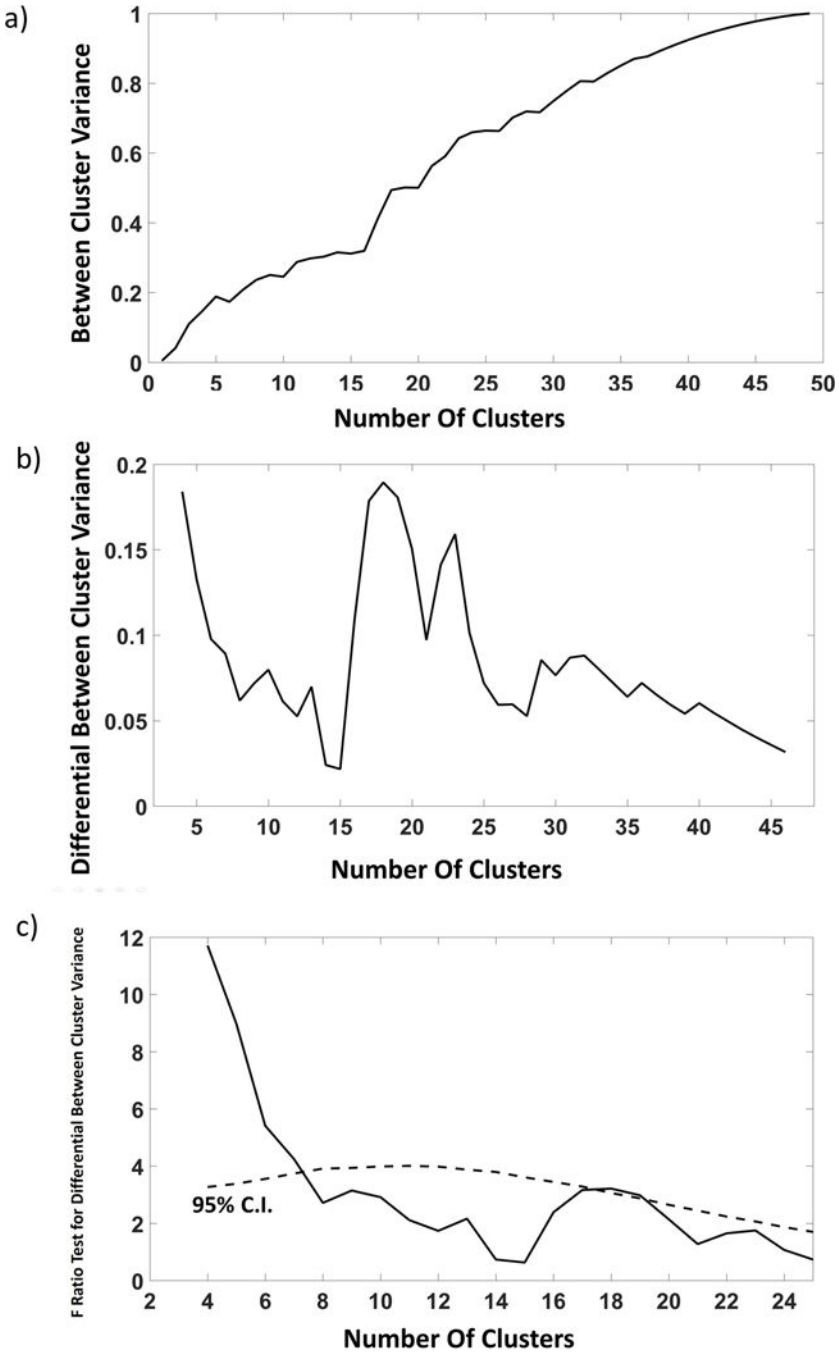

Figure 8.

Steps of a procedure to determine whether the cluster classification of ROIs based on PReFx accounts for relative variations in volume across the same ROIs. (a) Proportion of the total between-ROIs volume variance that is accounted for by a PReFx-based classification of regions in different clusters (plotted as a function of number of clusters used for the classification). (b) Increments in between-cluster volume variance (steps of 4 clusters) plotted as a function of number of clusters used for the classification (this is equivalent to computing a smoothed derivative of the function presented in (a); (c) Continuous line:

Results of an extra sum-of-square analysis (F ratio) of the increments in volume variance accounted for by the PReFx clusters obtained by increasing the number of cluster. The F ratio involves considering the DFs for the numerator (always 3, the number of the steps minus one) and denominator (49 minus the number of clusters entered in the predictive model based on the cluster classification). Dashed line: 95% confidence interval for this F ratio computed on the basis of a Monte Carlo procedure.

Table 1

Demographic, neuropsychological, and physiological characteristics of the participants.

	All (N=47)		Younger (<48) (N=23)		Older (>48) (N=24)		*t*-test (2-tailed)	
Females: Males	**24: 23**		**11: 12**		**13: 11**			
	Mean	**SD**	**Mean**	**SD**	**Mean**	**SD**	**p**	
Age	47.58	17.51	32.05	9.19	62.47	7.76	0.000	***
Education (years)	17.28	2.23	16.52	1.95	18.00	2.28	0.021	*
Weight (Lbs)	185.11	41.30	185.29	43.60	184.93	39.90	0.976	
Height (Inches)	68.08	3.57	67.89	3.33	68.26	3.85	0.726	
BMI	28.01	5.55	28.20	5.92	27.82	5.29	0.820	
BDI	2.55	3.31	3.13	2.69	2.00	3.79	0.243	
mMMS	55.77	1.22	55.61	1.31	55.92	1.14	0.394	
Heart Rate	70.12	8.42	69.85	9.38	70.39	7.59	0.830	
Systolic BP	130.58	13.73	129.58	14.28	131.54	13.42	0.629	
Diastolic BP	78.87	8.03	79.51	7.39	78.26	8.71	0.598	
Pulse Pressure	51.71	10.15	50.07	10.23	53.28	10.03	0.282	

+ p < .10,

* p < .05,

** p < .01,

*** p < .001. BMI=body mass index; BDI=Beck's depression inventory; BP=blood pressure; mMMS= modified Mini Mental Status Exam

Table 2

FreeSurfer regions analyzed, average volume, optical voxels, and percent (%) volume explored with optical recordings

	Left Hemisphere			Right Hemisphere		
ROI	**Average volume (mm^3)**	**Optical voxels (mm^3)**	**Percent optically sampled**	**Average volume (mm^3)**	**Optical voxels (mm^3)**	**Percent optically sampled**
Banks of Sup. Temp. S.	2505	501	20	2440	590	24
Caudal Mid. Frontal	6543	3691	56	6032	2226	37
Cuneus	2860	532	19	3167	464	15
Frontal Pole	12610	2934	23	15174	3324	22
Inf. Parietal	11191	1617	14	10659	1680	16
Inf. Temporal Gyrus	12008	1387	12	12074	1417	12
Lat. Occipital	7437	878	12	7217	934	13
Lat. Orbitofrontal	4832	647	13	4983	643	13
Med. Orbitofrontal	11176	2464	22	12395	2532	20
Mid. Temporal	3514	1252	36	4067	1252	31
Paracentral Gyrus	4868	2245	46	4079	1579	39
Pars Opercularis	2205	357	16	2587	384	15
Pars Orbitalis	3642	917	25	4207	1064	25
Pars Triangularis	1961	342	17	2260	340	15
Pericalcarine	10262	3721	36	9829	4008	41
Postcentral Gyrus	13774	5710	41	13449	5999	45
Precentral Gyrus	9598	2534	26	10027	2801	28
Precuneus	15449	5129	33	15848	5798	37
Rostral Mid. Frontal	22578	8458	37	21622	9313	43
Sup. Frontal	13380	5423	41	13480	6111	45
Sup. Parietal	11912	3478	29	11361	2396	21
Sup. Temporal	11273	2125	19	10417	1493	14
Supramarginal	797	126	16	1084	147	14
Temporal Pole	2471	299	12	2249	262	12
Transverse Temporal	1194	663	56	930	323	35

Sup. = Superior; Inf. = Inferior; Mid. = Middle; Lat. = Lateral; Med. = Medial; Temp. S. = Sulcus